A Doctoral Thesis

Regulatory mechanism of the *SRC* oncogene expression mediated by TGF-β-responsive enhancer

（TGF-β 応答性エンハンサーを介したがん遺伝子 *SRC* の発現制御機構）

Graduate School of Science
Department of Oncogene Research
Research Institute for Microbial Diseases
Osaka University

Soshi Noshita

August 2023

Table of contents

Abbreviations

- AP-1: Activator protein-1
- BRCA: Breast cancer
- CDK: Cyclin-dependent kinase
- CDKN: Cyclin-dependent kinase inhibitor
- CHX: Cycloheximide
- COSMIC: Catalogue of somatic mutations in cancer
- CRISPR: Clustered regularly interspaced short palindromic repeats
- CRISPRi: CRISPR interference
- Cas9: CRISPR-associated protein 9
- ChIP: Chromatin immunoprecipitation
- ChIP-Seq: ChIP-Sequence
- ChIP-on-chip: ChIP with DNA microarray
- Chr: Chromatin
- Csk: C-terminal Src kinase
- ECM: Extracellular matrix
- EGF: Epidermal growth factor
- EMT: Epithelial-mesenchymal transition
- ERK: Extracellular signal-regulated kinase
- FAK: Focal adhesion kinase
- H3K4me1: Histone H3 4^{th} lysine mono-methylation
- H3K4me3: Histone H3 4^{th} lysine tri-methylation
- H3K27Ac: Histone H3 27^{th} lysine acetylation
- IP: Immunoprecipitation
- JNK: c-Jun N-terminal kinase
- Luc: Luciferase
- MAPK: Mitogen-activated protein kinase
- MLCK: Myosin light chain kinase
- MMP: Matrix metalloproteinase
- N.S.: Not significantly different
- NHEK: Normal human epidermal keratinocyte

- PCR: Polymerase chain reaction
- RT-PCR: Reverse transcription polymerase chain reaction
- qPCR: Quantitative polymerase chain reaction
- PI3K: phosphoinositide 3-kinase
- ROCK: Rho-associated protein kinase
- RTK: Receptor tyrosine kinase
- Rho: Ras homolog family member
- SBS: Smad binding site
- SD: Standard deviation
- SH2/3: Src homology domain 2/3
- SP1: Specificity protein 1
- TCGA: The Cancer Genome Atlas
- TGF-β: Transforming growth factor-β
- TGFBR (TβR): TGF-β receptor
- TSE: TGF-β-responsive SRC enhancer
- WT: Wild type
- cDNA: Complementary DNA
- dCas9: Deactivated Cas9
- gRNA: guide RNA
- mRNA: Messenger RNA
- miRNA: Micro RNA
- siRNA: Small interference RNA

Abstract

The non-receptor tyrosine kinase, SRC, plays a crucial role in regulating intracellular signaling pathways associated with cell proliferation, survival, adhesion, and motility. In various human cancers, SRC is overexpressed and/or hyperactivated and facilitates cancer progression by promoting invasion and metastasis. Overexpression of SRC was observed over two decades ago in human breast cancer. A current multi-omics study also revealed that SRC is overexpressed at the mRNA level and is an essential gene for breast cancer progression. However, the mechanisms underlying SRC overexpression remain poorly understood.

In this study, I focused on the molecular mechanisms of SRC expression and demonstrated that transforming growth factor-β (TGF-β) induces SRC expression at the transcriptional level by activating an intragenic SRC enhancer. In the human breast epithelial cell line MCF10A, TGF-β1 stimulation upregulated the *SRC1A* promoter, resulting in increased SRC mRNA and protein levels. Chromatin immunoprecipitation (ChIP)-sequencing analysis revealed that SMAD complex is recruited to three enhancer candidate regions located approximately15 kb upstream and downstream of the *SRC* promoter, with one of these enhancers capable of activating the *SRC* promoter in response to TGF-β. In addition, JUN, a member of the activator protein (AP)-1 family, also localizes to the enhancer and regulates TGF-β-induced SRC expression. We refer to the enhancer as TGF-β-responsive SRC Enhancer (TSE).

While SRC is overexpressed in various human cancers, the effects of increased SRC expression on cellular functions remain unclear. To elucidate the role of increased SRC expression, I next established TSE-mutant MCF10A cell lines using the CRISPR/Cas9 system. TGF-β-induced SRC expression was completely suppressed in these cell lines at both mRNA and protein levels. Importantly, TSE mutation did not affect TGF-β-induced cytostasis and epithelial–mesenchymal transition (EMT)-associated morphological changes. However, it decreased the SRC-mediated phosphorylation of focal adhesion kinase (FAK), and EMT-associated cell migration was reduced in the TSE mutant cell lines. Moreover, TGF-β-induced cell motility was recovered by bypassing TSE-mediated SRC expression with overexpressing wild-type SRC protein in ΔTSE cell lines. These results indicated that TSE-mediated SRC upregulation is crucial for FAK activation to maximize TGF-β-induced cell migration.

In summary, I demonstrated that a TGF-β-responsive enhancer upregulates SRC expression, and TGF-β-induced SRC expression is essential for EMT-associated cell migration (Figure). These findings suggest that the overexpression of SRC observed in a subset of human cancers may be induced by TGF-β secreted in the tumor microenvironment. Further investigation of the transcriptional

mechanisms of *SRC* may provide promising targets for anti-cancer drugs that prevent tumor invasion and metastasis.

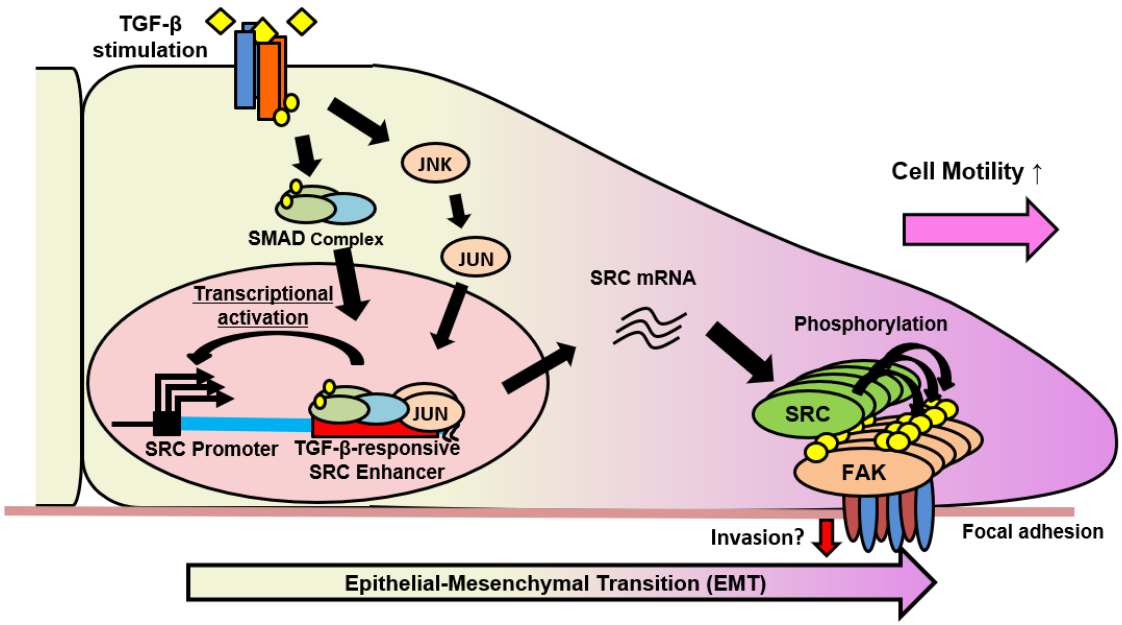

Figure. Schematic diagram of TSE-mediated SRC expression and upregulation of cell motility.

Publication List

Noshita, S., Kubo, Y., Kajiwara, K., Okuzaki, D., Nada, S., and Okada, M. (2023)

"A TGF-β-responsive enhancer regulates SRC expression and epithelial–mesenchymal transition-associated cell migration." *Journal of Cell Science*, jcs.261001., DOI: 10.1242/jcs.261001

General Introduction

1. Proto-oncogene *Src*

1.1. Structure and functions of Src

The *Src* gene is the first identified proto-oncogene and the first identified tyrosine kinase. The *Src* gene encodes non-receptor tyrosine kinase composed of several functional domains and residues (Yeatman, 2004). Src protein is composed of the SH3 domain, which can bind to proline-rich site; the SH2 domain, which can bind to phosphorylated tyrosine residue; a kinase domain, which contains a positive-regulatory phosphorylation site at Tyr419 (in humans); and a C-terminal regulatory tail, which contains a negative-regulatory phosphorylation site at Tyr530 (in humans) (Fig. G1A). The N-terminal region of Src has a myristoylation signal necessary for its membrane localization. The SH2 and SH3 domains are essential for the intra- and intermolecular interactions to regulate Src activity. When C-terminal Tyr530 is phosphorylated by Csk (Nada et al., 1991), phospho-Tyr530 residue binds to the SH2 domain, and the SH3 domain binds to the proline-rich linker between the SH2 domain and the kinase domain. Because of these intramolecular interactions, Src becomes the inactive conformation and the kinase activity is suppressed (Fig. G1B, Upper left). However, when phospho-Tyr530 residue is dephosphorylated by phosphatases (e.g., PTP1B), the conformation of Src loosens, and the SH2 and SH3 domains can be used for intermolecular interactions with other proteins, rather than intramolecular interactions. Due to the open conformation, Src can undergo the autophosphorylation of the positive-regulatory site at Tyr419 and acquire maximal kinase activity (Fig. G1B, Upper middle). By the action of these mechanisms, the activity of Src is strictly regulated in normal cells.

1.2. Src signaling pathway

Src is one of the most investigated signal proteins and many Src-mediated signaling pathways have been reported so far. Among these investigations, Src is activated either by extracellular stimulations (e.g., Receptor Tyrosine Kinase, RTK; Integrin) or intracellular stimulations (e.g. interaction with adapter proteins) (Guarino, 2010). Following these stimulations, Src modulates various cellular functions, including proliferation, growth, survival, adhesion, and migration (Fig. G1B). For example, Src regulates cell proliferation by activating the Ras/MAPK pathway, growth and survival by activating the PI3K/Akt pathway, adhesion by activating the Integrin/FAK pathway, and migration by activating the Rho/ROCK pathway (Guarino, 2010). Since Src regulates various cellular

functions, the activity of Src needs to be strictly regulated. Importantly, Src is overexpressed and/or activated in various human malignancies, implying that the dysregulation of Src plays a crucial role in tumor progression (Ishizawar and Parsons, 2004; RB and TJ, 2000; Verbeek et al., 1996; Wiener et al., 2003; Yeatman, 2004).

1.3. The role of Src in cancer progression

Src was originally discovered from the genome of the Rous sarcoma virus as "*v-Src* (*viral Src*)". Subsequently, the cellular counterpart of v-*Src* was identified and it is known as "*c-Src*" (*cellular Src*)" or simply "*Src*" nowadays. The notable feature of v-Src is the absence of the C-terminal regulatory tail. Because of this difference, v-Src activity is uncontrollable and constitutively "On" state (Collett and Erikson, 1978) (Fig. G1B, Upper right). The introduction of v-Src it cells is sufficient to transform them by accelerating Src signaling pathways and inducing chromosome abnormalities. Although Src is a proto-oncogene and constitutively active Src mutants can transform cells, *Src* is rarely mutated in human cancers (Yeatman, 2004). This evidence implies that Src mutants may not be involved in naturally occurring tumorigenesis. While c-Src itself is less oncogenic, numerous investigations have established that it facilitates the invasion and metastasis of cancer cells by regulating the turnover of focal adhesions, cytoskeletal remodeling, formation of invadopodia, and secretion of matrix metalloproteinases (MMPs) for the extracellular matrix (ECM) degradation (Guarino, 2010). Therefore, it is now considered that Src plays an important role in tumor progression rather than tumor initiation. In various human cancers, Src is overexpressed and/or hyperactivated and facilitates cancer progression by promoting invasion and metastasis; however, the mechanisms underlying Src dysregulation are poorly understood.

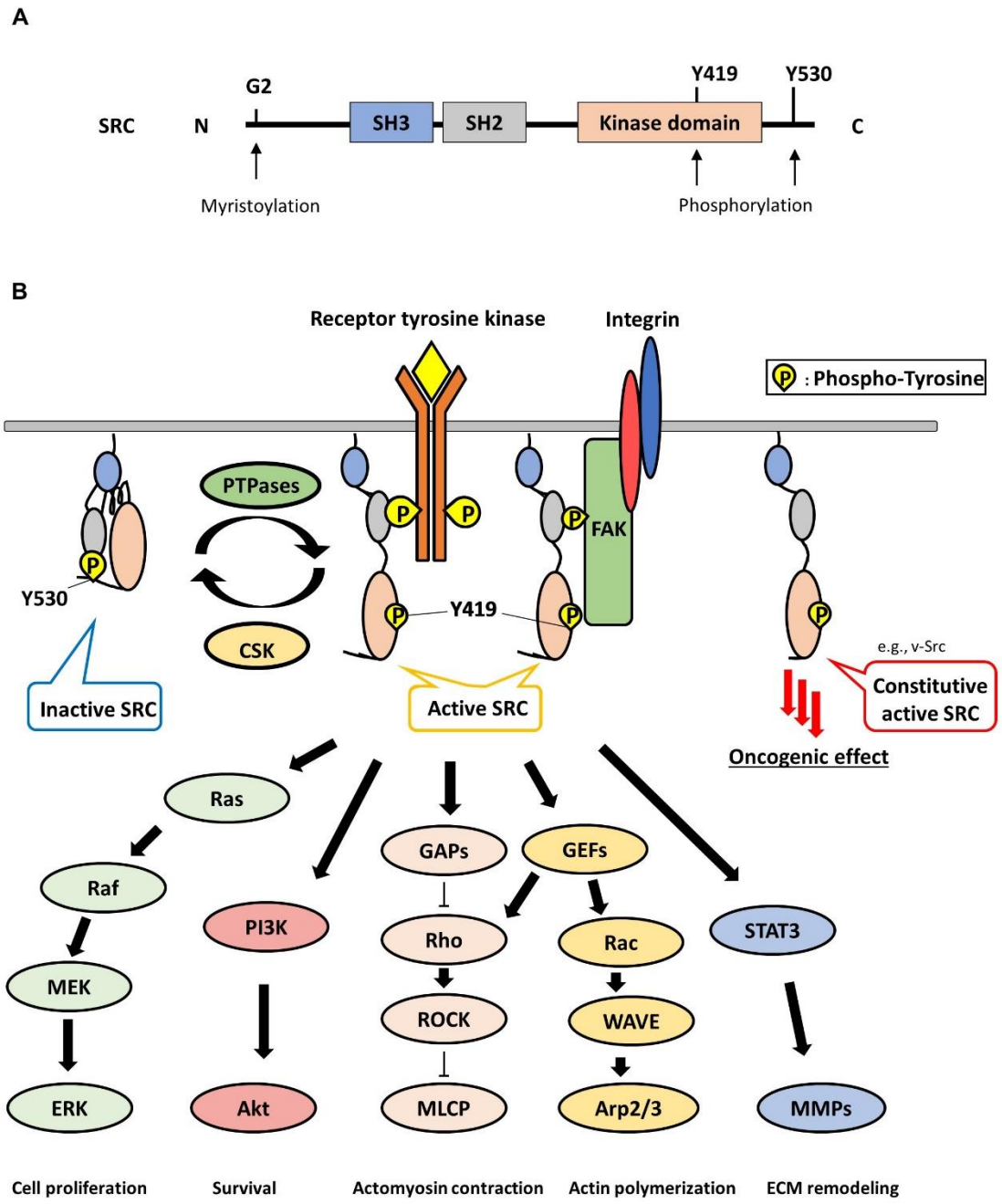

Figure G1. Regulatory mechanism of Src and Src signaling

2. Transforming Growth Factor-β (TGF-β)

2.1. Molecular mechanisms of TGF-β signaling pathway

Transforming Growth Factor-β (TGF-β) is a multifunctional cytokine that regulates morphogenesis, tissue homeostasis, wound repair, and so on (Massagué, 2012). TGF-β was originally identified as a cytokine with the ability to transform mouse fibroblast cells; however, further studies revealed that TGF-β has tumor-suppressive functions, and TGF-β is now considered one of the most important factors for inhibiting tumorigenesis (Colak and ten Dijke, 2017; Joan Massagué, 2008; Padua and Massagué, 2009). In the TGF-β signaling pathway, the type I and type II TGF-β receptors, which are serine/threonine kinases, are mainly involved in receiving TGF-β stimulation (Fig. G2). Once the TGF-β ligand binds to the type II TGF-β receptor, the receptor recruits the type I TGF-β receptor, and they form a hetero-tetrameric receptor complex composed of two type I receptors and two type II receptors. Subsequently, the type II TGF-β receptor phosphorylates the type I TGF-β receptor, and the activated type I TGF-β receptor phosphorylates various substrates to activate downstream signaling pathways (Massagué, 2012).

Canonical and non-canonical TGF-β signaling pathways are mediated by SMAD family proteins and non-SMAD proteins, respectively. In the canonical TGF-β/SMAD pathway, C-terminal serine residues of SMAD2 and SMAD3 are phosphorylated by activated type I TGF-β receptor (Fig. G2, Left). Phosphorylated SMAD2/3 form a heterotrimeric complex with SMAD4, and the SMAD complex translocates to the nucleus as a signal transducer. Subsequently, the SMAD complex acts as a transcription factor and regulates the expression of target genes by directly binding to regulatory gene sequences (Shi and Massagué, 2003). SMAD proteins can also regulate histone modification at enhancer regions cooperating with chromatin remodeling complex (Gaarenstroom and Hill, 2014). TGF-β-induced cellular changes are mainly regulated via SMAD proteins and transcription factors induced by SMAD proteins. In the non-canonical signaling pathway, TGF-β receptors can also initiate other signaling pathways, including various MAPKs (e.g., ERK, JNK, and p38), Rho/ROCK, and PI3K pathways (Colak and ten Dijke, 2017) (Fig. G2, Right).

2.2. Biological functions of TGF-β signaling pathway ~A dual role in cancer~

Basically, TGF-β regulates multiple cellular functions, including cell proliferation, survival, and motility, by activating or repressing the expression of related gene subsets. These functions are essential for maintaining tissue homeostasis, and dysfunction of the TGF-β signaling pathway

contributes to many diseases, including cancer. In normal cells, TGF-β stimulation promotes cell cycle arrest by inducing p15 (CDKN2B) and p21 (CDKN1A), which inhibit CDK4/6 and CDK2, respectively. In addition, TGF-β suppresses c-MYC expression and these transcriptional changes result in the downregulation of cell proliferation (Joan Massagué, 2008). TGF-β stimulation also promotes apoptosis in pre-malignant epidermal cells but not in normal epidermal cells, indicating that TGF-β can autonomously inhibit tumorigenesis in the cell. Importantly, the TGF-β signaling pathway is frequently abolished by mutations in *SMAD4* or *TGFBR2* in human colorectal and pancreatic cancers (Joan Massagué, 2008; Levy and Hill, 2006). Thus, TGF-β is a powerful tumor suppressor, and TGF-β receptors and SMAD proteins are considered one of the most important tumor suppressor genes.

Interestingly, however, an intact TGF-β/SMAD pathway is retained in some types of cancers (e.g., breast cancer, melanoma, and glioma), and TGF-β promotes tumor progression, including invasion and metastasis (Colak and ten Dijke, 2017; Massagué, 2012). In late-stage cancers, TGF-β strongly induces a dramatic cellular change called epithelial-mesenchymal transition (EMT). During EMT, epithelial cells lose cell–cell adhesion and apical-basal polarity and acquire mesenchymal traits, such as higher cell motility and invasiveness (Fuxe et al., 2020). In many cases, SMAD proteins regulate the expression of EMT-related transcription factors, including SNAI1/2, ZEB1/2, and TWIST1, and these transcription factors facilitate cellular phenotypic changes. Although the basic molecular mechanisms of the TGF-β signaling pathway are common in normal cells and cancer cells, TGF-β plays a dual role as a tumor suppressor and promoter. As TGF-β regulates various gene subsets and facilitates subsequent cellular changes, comprehensive studies, including gene expression, cell morphology, and cell functions, are important to understand the TGF-β signaling pathway in cancer progression comprehensively.

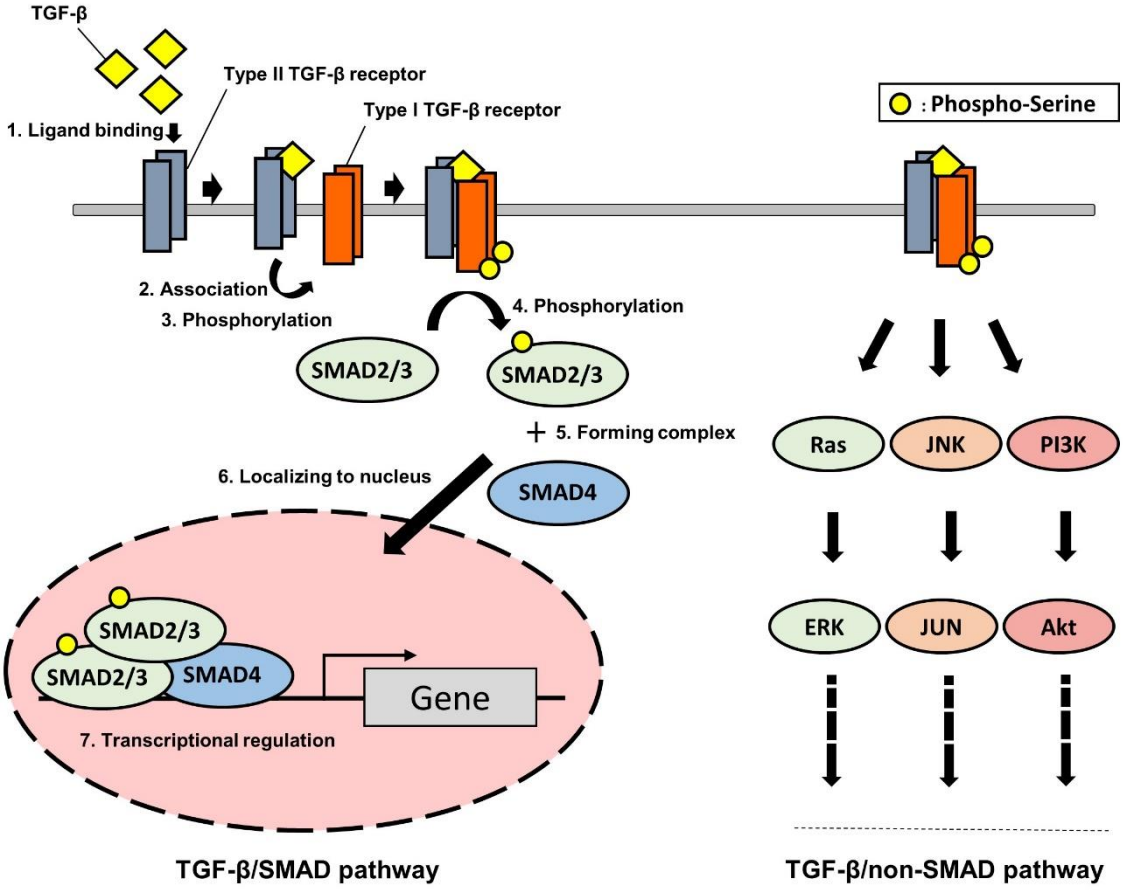

Figure G2. TGF-β/SMAD and non-SMAD signaling pathway

Introduction

The proto-oncogene SRC, a non-receptor tyrosine kinase, plays a pivotal role in regulating various cellular functions including proliferation, survival, adhesion, and migration. SRC facilitates the invasion and metastasis of cancer cells by accelerating their function (Guarino, 2010; Yeatman, 2004). SRC is overexpressed and/or activated in various human malignancies, implying that it plays a crucial role in tumor progression (Ishizawar and Parsons, 2004; RB and TJ, 2000; Verbeek et al., 1996; Wiener et al., 2003; Yeatman, 2004). SRC overexpression was first observed over two decades ago in human breast cancer (Verbeek et al., 1996). Furthermore, a recent multiomics study revealed that SRC is overexpressed at the mRNA level and is essential for breast cancer progression (López-Cortés et al., 2020). However, the mechanisms underlying the overexpression of SRC in breast cancer still remain unclear. In particular, the transcriptional regulation of *SRC* is poorly understood.

Transforming growth factor-β (TGF-β), a multifunctional cytokine, regulates multiple cellular functions, including cell proliferation, differentiation, and motility, to maintain tissue homeostasis (Massagué, 2012). TGF-β plays a dual role in cancer progression as a tumor suppressor and promoter. As a tumor suppressor, TGF-β induces cell cycle arrest and apoptosis in normal and pre-malignant cells. In cancer cells, however, TGF-β promotes tumor invasion and metastasis by inducing epithelial–mesenchymal transition (EMT) (Colak and ten Dijke, 2017; Padua and Massagué, 2009). During EMT, epithelial cells lose cell–cell adhesion and apical-basal polarity and acquire mesenchymal traits, such as cell motility and invasiveness (Fuxe et al., 2020). In addition to TGF-β, SRC promotes cell migration and invasion by regulating the turnover of focal adhesions, cytoskeletal remodeling, formation of invadopodia, and secretion of matrix metalloproteinases (MMPs) to degrade the extracellular matrix (ECM). Therefore, further studies on the relationship between TGF-β signaling and SRC should be conducted to better understand cancer progression.

In previous studies, we found that ARHGEF5, a Rho guanine nucleotide exchange factor, is upregulated and promotes cell migration by activating the Rho-ROCK pathway during TGF-β-induced EMT in the human breast epithelial cell line, MCF10A (Komiya et al., 2016; Kuroiwa et al., 2011). Moreover, we observed that SRC facilitates the activation of ARHGEF5, leading to cell invasion and tumor growth (Komiya et al., 2016). In addition to these findings, we found that SRC protein and mRNA levels increased, coinciding with TGF-β-induced EMT. However, the mechanisms by which TGF-β signaling regulates SRC gene expression remain unknown. In addition, the effects of TGF-β-induced SRC expression on cellular functions pooly understood.

To address these issues, I investigated the molecular mechanisms underlying TGF-β-induced SRC expression, and found that a TGF-β-responsive enhancer, which is located in the *SRC* intragenic region, upregulated SRC promoter activity via the TGF-β/SMAD and/JNK/JUN pathways. Based on these findings, I established the enhancer-deficient cell lines and demonstrated that elevated SRC expression is essential for promoting EMT-associated cell motility by phosphorylating Focal adhesion kinase (FAK). These findings help to elucidate how SRC is overexpressed in various human cancers and provide valuable insights into how SRC overexpression contributes to tumor progression.

Results

SRC protein and exon1A transcripts are increased during TGF-β-induced EMT

The normal human breast epithelial cell line, MCF10A, was used to analyze SRC expression during EMT. TGF-β stimulation of MCF10A cells induced morphological changes, such as the reduction of E-cadherin-mediated cell–cell adhesion and the formation of stress fibers (Fig. 1A). In addition, a switch from E-cadherin to N-cadherin was observed, indicating that EMT had been induced in these cells (Fig. 1B). During EMT, SRC protein and mRNA levels were elevated 2- to 4-fold in a time-dependent manner (Fig. 1B and C). TGF-β-induced SRC expression was also observed in the triple-negative breast cancer cell line BT-549 (Fig. 1D and E). SRC has been reported to be overexpressed in renal cancer cell lines by downregulating miR-205, which targets and degrades SRC mRNA (Majid et al., 2011). To verify whether TGF-β affects the stability of SRC mRNA, I assessed the degradation rate of SRC mRNA in the presence or absence of TGF-β by arresting transcription using actinomycin D. The results revealed that TGF-β treatment did not significantly affect the stability of *SRC* mRNA (Fig. 2A), suggesting that TGF-β regulates *SRC* expression primarily at the transcriptional level.

Two types of *SRC* transcripts encode identical SRC proteins whose expression is regulated by two different promoters: SRC1A and SRC1α (Bonham et al., 2000; Ritchie et al., 2000) (Fig. 2B). Reverse transcription PCR (RT-PCR) analysis showed that SRC exon1A transcripts, but not SRC exon1α transcripts, were increased by TGF-β stimulation, implying that the SRC1A promoter was selectively activated (Fig. 2C). Previous studies have revealed that SRC1A promoter activity is dependent on the SP1 transcription factor, and an increased SP1 expression results in SRC1A promoter activation and SRC expression (Liu et al., 2018; Ritchie et al., 2000). However, in the present study, TGF-β stimulation did not induce SP1 expression in MCF10A cells (Fig. 2D). Together, these observations indicate that there may be unknown regulatory mechanisms involved in TGF-β-induced SRC transcription.

SRC expression is directly regulated via the TGF-β/SMAD canonical signaling pathway

To identify the signaling pathways and transcription factors that induce *SRC* promoter activation, I examined the TGF-β/SMAD signaling pathway. The type I TGF-β receptor inhibitor LY364947 inhibited C-terminal phosphorylation of SMAD2 and TGF-β-induced SRC protein expression (Fig.

3A). I also established SMAD4-knockout (KO) MCF10A cells using CRISPR/Cas9. TGF-β failed to induce SRC expression at the protein and mRNA levels in SMAD4-KO cells, indicating that the SMAD4 is essential for regulating SRC transcription (Fig. 3B and C). As TGF-β drives the EMT process by inducing various EMT-associated transcription factors (Fuxe et al., 2020), I also examined the contribution of TGF-β-induced factors. Although inhibition of *de novo* protein synthesis using cycloheximide reduced basal levels of SRC mRNA, TGF-β-induced elevation of SRC transcription was observed even in the presence of cycloheximide and was suppressed by LY364947 (Fig. 3D). These results suggest that the pre-existing TGF-β/SMAD pathway regulates SRC transcription.

SRC intragenic enhancer upregulates *SRC* promoter activity by TGF-β stimulation

I then attempted to identify the genomic region contributing to TGF-β-induced SRC transcription using chromatin immunoprecipitation (ChIP) with H3K4me3, H3K27Ac, SMAD2, or SMAD3 antibodies. ChIP-Seq results showed the recruitment of SMAD2 and SMAD3 to three regions ~15 kb upstream and downstream of the *SRC* promoter, respectively (Fig. 4A and B). Moreover, these regions are marked by H3K27Ac, an epigenetic modification frequently observed at active enhancer sites (Gaarenstroom and Hill, 2014). I refer to these possible regulatory regions as enhancers A, B, and C, respectively, from the upstream *SRC* loci. To assess the contribution of these regions to TGF-β-induced *SRC* promoter activation, I measured the activity of these enhancers using a luciferase reporter assay. The results showed that Enhancer B could upregulate *SRC* promoter activity following TGF-β stimulation (Fig. 5A). Next, I conducted motif analysis using the JASPAR database (Castro-Mondragon et al., 2022) and found that there are two putative Smad-binding sites (SBS#1 and SBS#2) in enhancer B. To confirm the TGF-β-responsive ability of enhancer B, I introduced mutations into these SBSs by 1 bp substitution or truncation, so that they are not predicted as the Smad-binding site (Fig. 5B). These mutations reduced TGF-β-induced *SRC* promoter activity, even when another SBS was intact (Fig. 5C and D). These data suggest that the two SBSs in enhancer B are required to upregulate of *the SRC* promoter activity. Hereafter, I refer to enhancer B as TGF-β-responsive SRC enhancer (TSE).

SRC promoter activity is also regulated by the TGF-β/JNK/JUN axis

In addition to SMAD, various transcription factors are required for TGF-β-induced gene expression (Massagué, 2012). Previous studies highlighted the critical role of the AP-1 transcription factor, which consists of JUN and FOS family proteins, in breast cancer invasion (Sundqvist et al.,

2018; Sundqvist et al., 2020). TGF-β stimulation activates JUN by phosphorylating serine residues via the TGF-β/JNK axis. Moreover, JUN family proteins directly interact with SMAD proteins to regulate downstream gene expression (Liberati et al., 1999), and ChIP-on-chip analysis has revealed enrichment of the AP-1 motif (Koinuma et al., 2009). Consistent with these findings, motif enrichment analysis using ChIP-Seq for SMAD2 in the presence of TGF-β indicated the presence of AP-1-related motifs at the SMAD complex-binding site (Fig. 6A). Furthermore, overlap analysis revealed that over 70% of the SMAD complex-binding regions overlapped with JUN-binding regions (Fig. 6B). ChIP-Seq and qPCR analyses also revealed the co-localization of SMAD2/3/4 and JUN in the TSE (Fig. 6C and D). Furthermore, the luciferase reporter assay demonstrated that TGF-β-induced SRC promoter activity was decreased by the AP-1 binding site mutation in TSE (Fig. 6E).

To further verify the involvement of the JNK/JUN signaling pathway in the regulation of SRC transcription, I examined the effects of JNK inhibitor treatment and JUN protein knockdown. TGF-β stimulation induced the expression and phosphorylation of JUN protein, and the the JNK inhibitor SP600125 inhibited JNK-mediated phosphorylation of JUN and reduced TGF-β-induced SRC expression (Fig. 7A and B). Moreover, JUN knockdown reduced TGF-β-induced SRC expression (Fig. 7C-E). These findings demonstrate that the TGF-β/JNK/JUN axis synergistically regulates *SRC* promoter activity.

TSE is essential for TGF-β-induced SRC expression and activation

Although many studies have reported that endogenous SRC expression is upregulated in various human cancers, the detailed effects of SRC overexpression on cellular functions are poorly understood. Then, to analyze the effects of TGF-β-induced SRC expression on cellular function, I tried to establish TSE-mutant MCF10A cell lines using the CRISPR/Cas9 system. The target sequence of the gRNA is the SBS#1 region of TSE. The *SRC* gene is located at chr.20 in the human genome, and MCF10A cells contain three chr.20s (chr.20 trisomy). Hence, I screened the clones with TSE-mutant on all chr.20, and obtained two clones (Fig. 8). In these cell lines, TGF-β-induced SRC expression was completely suppressed at both mRNA and protein levels (Fig. 9A-C). For further characterization of the TSE, I used the CRISPR interference (CRISPRi) system to repress the TSE activity and analyzed the TGF-β-induced SRC expression. As in CRISPR/Cas9-based mutation, TGF-β-induced SRC expression was also suppressed by the inhibition of TSE activity using CRISPRi (Fig. 9D and E). These results verify that TSE-mediated SRC upregulation occurs via the endogenous SRC transcriptional machinery. Notably, although the total amount of active SRC (pY419) was increased by TGF-β stimulation in

wild-type cells (Fig. 9B), the ratio of active SRC to total SRC did not change in either wild-type or TSE-mutant cells (Fig. 9F). These results suggest that TGF-β-induced SRC activation is mainly attributable to the upregulation of TSE-mediated SRC expression. In the following studies, I analyzed the TGF-β-associated cellular functions using these cell lines.

TGF-β-induced cytostasis and EMT-associated morphological changes occur even in the absence of TSE

In normal cells, TGF-β stimulation promotes cell cycle arrest by inducing p15 (CDKN2B) and p21 (CDKN1A) and suppressing c-MYC expression; these transcriptional changes result in the downregulation of cell proliferation. Nevertheless, SRC activation promotes cell proliferation by activating the ERK/MAPK pathway. Based on these studies with conflicting findings, the effect of TGF-β-induced SRC expression on cell proliferation remains unclear. To clarify this, I conducted a cell proliferation assay in the presence or absence of TGF-β in wild-type and TSE mutant MCF10A. The cell proliferation assay showed that a growth arrest effect was observed at the same ratio in both the wild-type and TSE-mutant cell lines, implying that TSE-mediated SRC expression did not significantly affect cell proliferation (Fig. 10). This result indicates that cell proliferation is more strongly regulated by TGF-β signaling rather than SRC activity.

Previous studies have shown that constitutively active SRC (e.g. v-Src, SrcY527F mutant) disrupts cell–cell contacts by directly phosphorylating E-cadherin and activating the SRC/FAK/ERK/MLCK/myosin pathway, resulting in the induction of EMT (Avizienyte and Frame, 2005; Avizienyte et al., 2004; Fujita et al., 2002; Webb et al., 2004). However, another study revealed that endogenous SRC activation is not necessary for TGF-β-induced EMT (Maeda et al., 2006). To elucidate the role of SRC in EMT, I evaluated the effects of TGF-β-induced SRC activation on EMT using a TSE-mutant MCF10A cell line. Immunoblot analysis revealed that the TSE mutation did not significantly affect the repression of E-cadherin or the induction of vimentin expression (Fig. 11A). In addition, EMT-associated cellular traits, including a reduction in E-cadherin-mediated cell–cell adhesion and the formation of stress fibers, were observed in both the wild-type and TSE mutant cell lines (Fig. 11B). To further characterize the relationship between EMT associated events and SRC activity, I evaluated the effects of SRC inhibition on EMT marker expression (Fig. 11C) and cell morphology (Fig. 11D and E) induced by TGF-β stimulation. Notably, the SRC inhibitor did not significantly affect the repression of E-cadherin or the induction of vimentin expression, consistent with our findings in the TSE-deficient cell line (Fig. 11A). A previous study showed that SMAD

complex and SNAI1 directly bind to the E-cadherin promoter and repress its expression (Vincent et al., 2009). I also found that TGF-β stimulation induced fibroblast-like morphological change in the presence of dasatinib (Fig. 11D). Furthermore, TGF-β-induced reduction of E-cadherin-mediated cell–cell adhesion was also observed even when SRC activity was inhibited (Fig. 11E). Importantly, I also found E-cadherin accumulation at the contact site of the cells (Fig. 11E, white arrowheads in the middle right panel). Previous studies have consistently shown that SRC-mediated endocytosis and degradation are required for the distribution of E-cadherin to the epithelial cell membrane (Balzac et al., 2005; Fujita et al., 2002). These findings suggest that EMT-associated morphological changes and gene expressions are predominantly regulated by TGF-β signaling and the contribution of SRC activity is relatively small. However, the increased TGF-β-induced SRC activity at the endogenous level is essential for completing morphological changes, including the reduction of E-cadherin-mediated cell–cell adhesion in MCF10A cells.

TSE regulates EMT-associated cell motility by upregulating SRC-mediated FAK phosphorylation

Finally, I investigated the effects of TSE-mediated SRC upregulation on EMT and identified proteins phosphorylated by SRC. Immunoblot analysis using an anti-phospho-tyrosine antibody (pY1000) revealed an increase in the phosphorylation of ~130 kDa proteins upon TGF-β stimulation in the wild-type cell line, but not in the TSE mutant cell lines (Fig. 12A). This suggests that TSE-mediated SRC upregulation results in the phosphorylation of these proteins. I examined several tyrosine-phosphorylated proteins that have previously been reported as SRC substrates (Guarino, 2010) and found that SRC-mediated phosphorylation of FAK was significantly reduced by the TSE mutation and CRISPRi-based inhibition of the TSE activity (Fig. 12B-E). Importantly, the FAK inhibitor Y15, which selectively interacts with Y397 in FAK and inhibits autophosphorylation of this residue (Golubovskaya et al., 2008), suppressed SRC-Y419 phosphorylation and subsequent FAK-Y576/577 phosphorylation (Westhoff et al., 2004) (Fig. 12F). These results suggest that TGF-β-induced SRC expression promotes the formation and activation of the SRC/FAK circuit.

Since SRC/FAK signaling plays a central role in cell migration (Avizienyte and Frame, 2005; Guarino, 2010; Le Coq et al., 2022; Westhoff et al., 2004; Yakymovych et al., 2022), I subsequently examined the effects of TSE-mediated SRC expression and activation on cell motility using a wound healing assay. I performed a wound healing assay using inhibitors of type I TGF-β receptor (LY364947), SRC (dasatinib), and FAK (Y15). TGF-β-induced cell migration was inhibited by the

treatment of these inhibitors, suggesting that signaling pathways mediated by type I TGF-β receptor, SRC, and FAK are essential for cell migration in MCF10A (Fig. 13A and B). TGF-β-induced cell migration was consistently decreased in the TSE mutant cell lines, (Fig. 14A and B). Furthermore, TGF-β-induced cell motility was restored by the overexpression of the wild-type SRC protein in ΔTSE cell lines, which can bypass TSE-mediated SRC expression (Fig. 15A-C). These findings indicate that TSE-mediated SRC upregulation is crucial for TGF-β-induced cell migration via SRC/FAK signaling.

Discussion

I investigated the mechanisms underlying TGF-β-induced upregulation of SRC in MCF10A cells and identified a TSE that induces the transcriptional activation of the *SRC* promoter via the TGF-β/SMAD and TGF-β/JNK/JUN signaling pathways. Since SRC has an oncogenic potential, its expression and activity are tightly regulated by post-transcriptional and post-translational pathways. During post-transcriptional regulation, miRNAs directly bind to SRC mRNA, resulting in its degradation and translational inhibition (Majid et al., 2011; Okuzaki et al., 2020; Oneyama and Okada, 2015; Wang et al., 2014). In post-transcriptional regulation, the specific activity of SRC is regulated by C-terminal regulatory phosphorylation (Nada et al., 1991; Okada, 2012), and its protein level is regulated by degradation via the lysosome (Tsai et al., 2019) and proteasome (Kim et al., 2004; Mukhopadhyay et al., 2016) systems, or by excretion througth small extracellular vesicles (Tanaka et al., 2020). In this study, I focused on the transcriptional regulation of *SRC*. This is the first report demonstrating the transcriptional regulation of *SRC* induced by TGF-β-responsive enhancers.

According to the COSMIC database, SRC is overexpressed in various human cancers; however, mutations in *SRC* are rare (Fig. 16A). Additionally, The Cancer Genome Atlas (TCGA) database analysis revealed that SRC is significantly overexpressed in human breast cancer (Fig. 16B). In colorectal and pancreatic cancers, the TGF-β signaling pathway is frequently abolished by mutations in *SMAD4* or *TGFBR2* (Joan Massagué, 2008; Levy and Hill, 2006). In contrast, TGF-β/SMAD signaling machinery is preserved in breast cancer (Joan Massagué, 2008). Furthermore, TGF-β signaling plays a pivotal role in promoting tumor cell invasion and bone metastasis in breast cancer (Deckers et al., 2006; Sundqvist et al., 2018; Sundqvist et al., 2020). These studies with our findings suggest a possible link between the upregulation of TGF-β signaling and SRC, particularly in breast cancer. Notably, TCGA analysis revealed that SRC was, on average, 1.8-fold overexpressed in patient-derived tissues (Fig 16B); however, SRC was not overexpressed in various breast cancer cell lines compared to the normal breast epithelial cell line MCF10A (Fig 16C). These results imply that further *in vivo* investigations are needed for a deeper understanding of the mechanisms underlying SRC overexpression in human cancer tissues, and our findings contribute to elucidating this.

A previous study revealed that TGF-β stimulation rapidly results in 5- to 10-fold activation of SRC in HEK293T, MEF, and PC3U cells, independent of the type I TGF-β receptor activity (Yakymovych et al., 2022). However, in MCF10A cells, SRC was not significantly activated by short-term TGF-β stimulation (Fig 17A and B). In addition, TGF-β-induced SRC activation depends on the

TGF-β/SMAD signaling pathway (Fig. 3A and B), and the total amount of active SRC was decreased in TSE-mutant MCF10A (Fig. 9B). Moreover, I showed that TGF-β-induced cell migration depended on the activity of type I TGF-β receptor, SRC, and FAK in MCF10A cells (Fig. 13A and B). These findings suggest that the TGF-β/SMAD signaling pathway and TSE-mediated SRC expression, rather than the type II TGF-β receptor dependent SRC activation, are essential for TGF-β-induced cell motility, at least in the MCF10A cell line.

Additionally, we have previously reported that TGF-β2 stimulation induces SRC activation by upregulating the SRC scaffolding protein, CASL, without upregulating SRC expression in primary human trabecular meshwork cells (Tsukamoto et al., 2019). Hence, the cell-type specificity determining whether TGF-β can induce SRC expression needs further elucidation. In this study, I showed that the AP-1 family protein JUN and SMAD bind to the TSE, activating the *SRC* promoter. AP-1, in combination with EGF signaling, plays an essential role in regulating the transcriptional program of SMAD and promotes TGF-β-induced invasiveness by cooperating with SMAD in breast cancer cell lines expressing ΔNp63 (Sundqvist et al., 2020). Consistent with this study, I found that co-stimulation with TGF-β and EGF induced SRC expression in normal human epidermal keratinocytes (NHEK) expressing ΔNp63 (Fig. 18A-C). These results imply that the cooperative mechanisms of SMAD and AP-1 may determine the cell-type specificity of TGF-β-induced SRC expression. Additionally, TSE contains epigenetic modifications of H3K4me1 without H3K27Ac, which represents a poised enhancer in the basal state of MCF10A and NHEK (Fig. 18D). This suggests that cell type-specific epigenetic states may also contribute cell type-specificity in TGF-β-induced SRC expression.

I also found that TSE-mediated SRC expression was crucial for increased FAK phosphorylation and TGF-β-induced cell motility. SRC/FAK signaling accelerates tumor invasiveness by regulating integrin-mediated cell adhesion, cell motility, and extracellular matrix degradation. Therefore, the TSE-mediated activation of the SRC/FAK circuit may promote EMT-associated cancer cell migration and invasion. Although the SRC protein regulates multiple cellular functions, TSE-mediated SRC expression did not promote cell proliferation or EMT-associated morphological change in MCF10A cells. This result implies that SRC does not always activate every downstream signaling pathway and subsequent cellular functions; some functions are predominantly regulated via the TGF-β signaling pathway in normal cells. When cancer cells evade the tumor suppressive effect of TGF-β, SRC might coordinate tumor invasion and metastasis by promoting cell motility and secreting matrix

metalloproteinases that degrade the extracellular matrix.

As SRC is a key protein in tumor progression, various small-molecule inhibitors of SRC have been developed for anti-cancer therapy (Mayer and Krop, 2010). However, ATP-competitive SRC inhibitors induce conformational changes in SRC, leading to stable interactions with FAK at focal adhesions. A subsequent reduction in the inhibitor concentration enables SRC to readily phosphorylate FAK and paradoxically activate the FAK-Grb2-Erk signaling pathway (Higuchi et al., 2021). In this study, I demonstrated that inhibiting TGF-β-induced SRC expression suppresses SRC activity and EMT-associated cell migration. This result suggests that the machinery of TSE-mediated SRC transcription can be a novel inhibitory target of SRC without causing unexpected effects, such as conformational changes in SRC.

In summary, I demonstrated that a TGF-β-responsive enhancer upregulates SRC expression, and TGF-β-induced SRC expression is essential for EMT-associated cell migration. These finding s suggest that the overexpression of SRC observed in a subset of human cancers may be induced by TGF-β secreted in the tumor microenvironment. Further investigation into the transcriptional mechanisms of *SRC* may provide promising targets for anti-cancer drugs that prevent tumor invasion and metastasis.

Materials and Methods

Cell culture

MCF10A cells were cultured in DMEM/F12 (Nacalai Tesque) supplemented with 5% horse serum (Gibco), 20 ng/mL EGF (PeproTech), 0.5 μg/mL hydrocortisone (Sigma), 10 μg/mL insulin (Wako), 100 ng/mL Cholera toxin (Bio Academia), and a penicillin-streptomycin solution (Nacalai Tesque). MCF7, T47D, MDA-MB-231, and Hs578T cells were cultured in DMEM supplemented with 10% fetal bovine serum (FBS). BT-549 cells were cultured in RPMI1640 (Nacalai Tesque) containing 10% FBS, 0.023 U/mL insulin (Wako), and a penicillin-streptomycin solution (Nacalai Tesque). Normal Human Epidermal Keratinocyte (NHEK) cells were purchased from PromoCell and cultured in keratinocyte growth medium 2 (PromoCell). The cells were maintained in a CO_2 incubator at 37 °C and 5% CO_2. Recombinant Human TGF-β1 (CHO derived) was purchased from PeproTech.

Antibodies and inhibitors

The following primary antibodies were used in this study: anti-v-Src (OP07) antibody was purchased from Sigma-Aldrich. Anti-phospho-Src family (pY416) (2101), anti-phospho-tyrosine (8954), anti-Smad2 (5339), anti-phospho-Smad2 (3108), anti-Smad3 (9523), anti-c-Jun (9165), anti-p-c-Jun (3270), anti-vimentin (5741), anti-p63-α (13109), anti-H3K4me3 (9751), and anti-H3K27c (8173) were purchased from Cell Signaling Technology. The anti-E-cadherin (610181), anti-N-cadherin (610920), and anti-FAK (610087) antibodies were purchased from BD Biosciences. Anti-GAPDH (32233), anti-SP1 (59), anti-Smad4 (7966), and anti-phospho-FAK (pY576/577) (21831) antibodies were purchased from Santa Cruz Biotechnology. Anti-phospho-FAK (pY397) (700255) antibody was purchased from Thermo Fisher Scientific.

The following inhibitors used in this study: TGFβR-I inhibitor LY364947 (S2805), JNK inhibitor SP600125 (S1460), and FAK inhibitor Y15 (S5321), were purchased from Selleck. Dasatinib (ab142050) was obtained from Abcam. Mitomycin C Solution (20898-21) was purchased from Nacalai Tesque. Actinomycin D (018-21264) was purchased from Wako.

Plasmid construction and gene transfer

The DNA sequences of enhancers A, B, and C were cloned by PCR using human genomic DNA as the template and subcloned into the pGV-B2 plasmid (Toyo B-Net). TSE mutants were generated using mutagenesis PCR. Wild-type SRC was generated by PCR using human cDNA and subcloned

into a pCX4 retroviral plasmid (generously donated by Dr. Akagi). Gene transfer of pCX4 was carried via retroviral infection. Plasmids were transfected using PEI MAX (Polysciences, Inc.). Primers used in this experiment are listed in Table 1. For establishing the CRISPRi system, each gRNA sequence was subcloned into pKLV2(Addgene, #67974). Stable gRNA expression was carried via lentiviral infection. siRNAs were purchased from Sigma-Aldrich and transfected using Lipofectamine RNAiMAX (Thermo Fisher Scientific). The siRNAs used in this study are listed in Table 2.

Immunoblotting

Cells were lysed with RIPA buffer (50 mM Tris-HCl [pH 7.4], 150 mM NaCl, 1% NP-40, 0.1% SDS, 1 mM EDTA, 0.5% sodium deoxycholate, 1 mM Na_3VO_4, 20 mM NaF, 1 mM PMSF, and protease inhibitor cocktail (Nacalai Tesque)), and debris were removed by centrifugation at 15,000× g for 10 min. Horseradish peroxidase-conjugated anti-mouse or anti-rabbit IgG (Zymed Laboratories Inc.) was used as the secondary antibody. All immunoblots were visualized using a Luminograph II System (Atto) and quantified using ImageJ software.

Immunofluorescence microscopy

The cells were grown on type I collagen-coated coverslips, fixed with 4% paraformaldehyde, and permeabilized with PBS containing 0.03% Triton X-100. The permeabilized cells were blocked with Blocking One (Nacalai Tesque) and incubated overnight with primary antibodies, followed by incubation with Alexa Fluor 488-conjugated phalloidin and Alexa Fluor 594-conjugated secondary antibodies. Immunostained samples were observed using an FV1000 confocal microscope (Olympus).

RNA isolation and qRT-PCR

Total RNA was isolated from the cells using a NucleoSpin RNA kit (Macherey-Nagel), and cDNA was prepared using the ReverTra Ace RT Master Mix (TOYOBO) according to the manufacturer's instructions. Real-time PCR was performed using a QuantStudio 5 Real-Time PCR System (Applied Biosystems) and THUNDERBIRD NEXT SYBR qPCR Mix (TOYOBO). Gene expression levels were normalized to GAPDH expression levels. The primers used for this analysis are listed in Table 3.

CRISPR/Cas9-based gene knockout and mutagenesis

Sequences of gRNA were designed using CRISPRdirect (DBCLS) and inserted into pX458. The

Target-gRNA containing pX458 was transfected into MCF10A cells using PEI MAX (Polysciences, Inc.). EGFP-positive cells were isolated the following day using a FACSAria III sorter (BD Biosciences). Genomic mutations were confirmed by immunoblotting and sequencing. Sequences of the gRNA and primers used for genotyping are listed in Table 4.

ChIP-Sequencing and data processing

Cells were cultured in a 15 cm dish to 80–90% confluence (approximately 2×10^7 cells), and one dish was used for immunoprecipitation. ChIP experiments were performed using the SimpleChIP Enzymatic Chromatin IP kit (9003, Cell Signaling Technologies) according to the manufacturer's instructions. The antibodies used for ChIP were anti-H3K4me3 (9751), anti-H3K27c (8173), anti-Smad2 (5339), anti-Smad3 (9523), anti-Smad4 (46535), anti-c-Jun (9165), and anti-JunB (3753) purchased from Cell Signaling Technology.

ChIP-seq libraries were prepared using the KAPA Hyper Preparation Kit. Sequencing was performed on a NovaSeq 6000 platform in 101+101 base paired-end mode. Illumina-TruSeq Adapter Trimming was performed on ChIP-seq reads, using cutadapt v2.7, discarding reads left with < 30 bp. ChIP-seq reads were aligned to the UCSC hg19 genome using Bowtie2 version 2.3.5.1. BigWig files were generated using the bamCoverage software of the deepTools package.

Peak call analysis, merge peak analysis and find motif analysis were performed by "findPeaks", "mergePeaks", and "findMotifsgenome.pl" programs, respectively in the HOMER version 4.11 package. ChIP-Seq data for H3K4me1 in MCF10A cells were obtained from the GSE85158 dataset. ChIP-seq data for SMAD2/3 in BT-549 cells were obtained from the GSE104352 dataset. ChIP-seq data for H3K4me1 and H3K27Ac in NHEK were obtained from GSE29611.

Luciferase Reporter Assay

For cell preparation, 5×10^4 cells were seeded in 48-well plates and cultured for 24 h. Cells were co-transfected with the pGV-B2 reporter vector and pRL-TK internal control vector for 20h. The following day, cells were stimulated with TGF-β for 24 h by refreshing the medium with or without 10 ng/mL TGF-β, and luciferase activity was assayed using a PicaGene Dual Sea Pansy Luminescence Kit (Toyo B-Net) according to the manufacturer's instructions.

Cell proliferation assay

For cell preparation, 1×10^3 cells were seeded in 96-well plates and cultured overnight. The following day, cells were stimulated with 10 ng/mL TGF-β and cultured for 1-4 days. Cell counting was performed using the Cell Count Reagent SF (Nacalai Tesque) before TGF-β stimulation (Day 0) and at each time point of 1-4 days after TGF-β stimulation. After adding the reagent to the medium, cells were incubated for 1 hour in a CO_2 incubator, and then the absorbance at 450 nm was measured using a Multiskan FC (Thermo Fisher Scientific).

Wound Healing Assay

For cell preparation, 3×10^4 cells were seeded into a 2-well silicone culture insert (ib80209, Ibidi) in a 35 mm dish and cultured overnight. Cells were treated with 10 μg/mL Mitomycin C containing medium for 2 h to stop cell proliferation, and then the culture inserts were removed. Cells were washed twice with PBS and cultured in a medium with or without 10 ng/mL TGF-β for 24 h. Cell images were taken at 0 h, 12 h, and 24 h.

Statistical analyses

All statistical analyses were performed using R version 4.0.3 and Microsoft Excel. One-way analysis of variance (ANOVA) with Tukey's post-hoc test was used for multiple group comparisons. Unpaired two-tailed t-tests were performed for comparisons between the two groups. A p-value less than 0.05 was considered significant. All data were obtained from at least three independent experiments.

Reference

Avizienyte, E. and Frame, M. C. (2005). Src and FAK signalling controls adhesion fate and the epithelial-to- mesenchymal transition. *Curr. Opin. Cell Biol.* **17**, 542–547.

Avizienyte, E., Fincham, V. J., Brunton, V. G. and Frame, M. C. (2004). Src SH3/2 Domain-mediated Peripheral Accumulation of Src and Phospho-myosin Is Linked to Deregulation of E-cadherin and the Epithelial-Mesenchymal Transition. *Mol. Biol. Cell* **15**, 2794–2803.

Balzac, F., Avolio, M., Degani, S., Kaverina, I., Torti, M., Silengo, L., Small, J. V. and Retta, S. F. (2005). E-cadherin endocytosis regulates the activity of Rap1: A traffic light GTPase at the crossroads between cadherin and integrin function. *J. Cell Sci.* **118**, 4765–4783.

Bonham, K., Ritchie, S. A., Dehm, S. M., Snyder, K. and Boyd, F. M. (2000). Alternative, human SRC promoter and its regulation by hepatic nuclear factor-1α. *J. Biol. Chem.* **275**, 37604–37611.

Castro-Mondragon, J. A., Riudavets-Puig, R., Rauluseviciute, I., Berhanu Lemma, R., Turchi, L., Blanc-Mathieu, R., Lucas, J., Boddie, P., Khan, A., Perez, N. M., et al. (2022). JASPAR 2022: The 9th release of the open-access database of transcription factor binding profiles. *Nucleic Acids Res.* **50**, D165–D173.

Colak, S. and ten Dijke, P. (2017). Targeting TGF-β Signaling in Cancer. *Trends in Cancer* **3**, 56–71.

Collett, M. S. and Erikson, R. L. (1978). Protein kinase activity associated with the avian sarcoma virus src gene product. *Proc. Natl. Acad. Sci. U. S. A.* **75**, 2021–2024.

Deckers, M., Van Dinther, M., Buijs, J., Que, I., Löwik, C., Van Der Pluijm, G. and Ten Dijke, P. (2006). The tumor suppressor Smad4 is required for transforming growth factor β-induced epithelial to mesenchymal transition and bone metastasis of breast cancer cells. *Cancer Res.* **66**, 2202–2209.

Ding, Q., Subramanian, I., Luckhardt, T. R., Che, P., Waghray, M., Zhao, X. K., Bone, N., Kurundkar, A. R., Hecker, L., Hu, M., et al. (2017). Focal adhesion kinase signaling determines the fate of lung epithelial cells in response to TGF-β. *Am. J. Physiol. - Lung Cell. Mol. Physiol.* **312**, L926–L935.

Fujita, Y., Krause, G., Scheffner, M., Zechner, D., Leddy, H. E. M., Behrens, J., Sommer, T. and Birchmeier, W. (2002). Hakai, a c-Cbl-like protein, ubiquitinates and induces endocytosis of the E-cadherin complex. *Nat. Cell Biol.* **4**, 222–231.

Fuxe, J., Mayor, R., Nieto, M. A., Puisieux, A., Runyan, R., Savagner, P., Thiery, J. P., Thompson, E. W., Theveneau, E. and Williams, E. D. (2020). Guidelines and definitions for research on

epithelial–mesenchymal transition. *Nat. Rev. Mol. Cell Biol.*

Gaarenstroom, T. and Hill, C. S. (2014). TGF-β signaling to chromatin: How Smads regulate transcription during self-renewal and differentiation. *Semin. Cell Dev. Biol.* **32**, 107–118.

Golubovskaya, V. M., Nyberg, C., Zheng, M., Kweh, F., Magis, A., Ostrov, D. and Cance, W. G. (2008). Site of Focal Adhesion Kinase Decreases Tumor Growth. 7405–7416.

Guarino, M. (2010). Src signaling in cancer invasion. *J. Cell. Physiol.* **223**, 14–26.

Higuchi, M., Ishiyama, K., Maruoka, M., Kanamori, R., Takaori-Kondo, A. and Watanabe, N. (2021). Paradoxical activation of c-Src as a drug-resistant mechanism. *Cell Rep.* **34**, 108876.

Ishizawar, R. and Parsons, S. J. (2004). C-Src and cooperating partners in human cancer. *Cancer Cell* **6**, 209–214.

Joan Massagué (2008). TGFβ in Cancer. *Cell* **134**, 215–230.

Kim, M., Tezuka, T., Tanaka, K. and Yamamoto, T. (2004). Cbl-c suppresses v-Src-induced transformation through ubiquitin-dependent protein degradation. *Oncogene* **23**, 1645–1655.

Koinuma, D., Tsutsumi, S., Kamimura, N., Taniguchi, H., Miyazawa, K., Sunamura, M., Imamura, T., Miyazono, K. and Aburatani, H. (2009). Chromatin Immunoprecipitation on Microarray Analysis of Smad2/3 Binding Sites Reveals Roles of ETS1 and TFAP2A in Transforming Growth Factor β Signaling. *Mol. Cell. Biol.* **29**, 172–186.

Komiya, Y., Onodera, Y., Kuroiwa, M., Nomimura, S., Kubo, Y., Nam, J. M., Kajiwara, K., Nada, S., Oneyama, C., Sabe, H., et al. (2016). The Rho guanine nucleotide exchange factor ARHGEF5 promotes tumor malignancy via epithelial-mesenchymal transition. *Oncogenesis* **5**,.

Kuroiwa, M., Oneyama, C., Nada, S. and Okada, M. (2011). The guanine nucleotide exchange factor Arhgef5 plays crucial roles in Src-induced podosome formation. *J. Cell Sci.* 1726–1738.

Le Coq, J., Acebrón, I., Rodrigo Martin, B., López Navajas, P. and Lietha, D. (2022). New insights into FAK structure and function in focal adhesions. *J. Cell Sci.* **135**,.

Levy, L. and Hill, C. S. (2006). Alterations in components of the TGF-β superfamily signaling pathways in human cancer. *Cytokine Growth Factor Rev.* **17**, 41–58.

Liberati, N. T., Datto, M. B., Frederick, J. P., Shen, X., Wong, C., Rougier-Chapman, E. M. and Wang, X. F. (1999). Smads bind directly to the Jun family of AP-1 transcription factors. *Proc. Natl. Acad. Sci. U. S. A.* **96**, 4844–4849.

Liu, W., Guo, T. F., Jing, Z. T., Yang, Z., Liu, L., Yang, Y. P., Lin, X. and Tong, Q. Y. (2018). Hepatitis B virus core protein promotes hepatocarcinogenesis by enhancing Src expression and

activating the Src/PI3K/Akt pathway. *FASEB J.* **32**, 3033–3046.

López-Cortés, A., Paz-y-Miño, C., Guerrero, S., Cabrera-Andrade, A., Barigye, S. J., Munteanu, C. R., González-Díaz, H., Pazos, A., Pérez-Castillo, Y. and Tejera, E. (2020). OncoOmics approaches to reveal essential genes in breast cancer: a panoramic view from pathogenesis to precision medicine. *Sci. Rep.* **10**, 1–21.

Maeda, M., Shintani, Y., Wheelock, M. J. and Johnson, K. R. (2006). Src activation is not necessary for transforming growth factor (TGF)-β-mediated epithelial to mesenchymal transitions (EMT) in mammary epithelial cells: PP1 directly inhibits TGF-β receptors I and II. *J. Biol. Chem.* **281**, 59–68.

Majid, S., Saini, S., Dar, A. A., Hirata, H., Shahryari, V., Tanaka, Y., Yamamura, S., Ueno, K., Zaman, M. S., Singh, K., et al. (2011). MicroRNA-205 inhibits Src-mediated oncogenic pathways in renal cancer. *Cancer Res.* **71**, 2611–2621.

Massagué, J. (2012). TGFβ signalling in context. *Nat. Rev. Mol. Cell Biol.* **13**, 616–630.

Mayer, E. L. and Krop, I. E. (2010). Advances in targeting Src in the treatment of breast cancer and other solid malignancies. *Clin. Cancer Res.* **16**, 3526–3532.

Mukhopadhyay, C., Triplett, A., Bargar, T., Heckman, C., Wagner, K. U. and Naramura, M. (2016). Casitas B-cell lymphoma (Cbl) proteins protect mammary epithelial cells from proteotoxicity of active c-Src accumulation. *Proc. Natl. Acad. Sci. U. S. A.* **113**, E8228–E8237.

Nada, S., Okada, M., MacAuley, A., Cooper, J. A. and Nakagawa, H. (1991). Cloning of a complementary DNA for a protein-tyrosine kinase that specifically phosphorylates a negative regulatory site of p60c-src. *Nature* **351**, 69–72.

Okada, M. (2012). Regulation of the Src family kinases by Csk. *Int. J. Biol. Sci.* **8**, 1385–1397.

Okuzaki, D., Yamauchi, T., Mitani, F., Miyata, M., Ninomiya, Y., Watanabe, R., Akamatsu, H. and Oneyama, C. (2020). c-Src promotes tumor progression through downregulation of microRNA-129-1-3p. *Cancer Sci.* **111**, 418–428.

Oneyama, C. and Okada, M. (2015). MicroRNAs as the fine-tuners of Src oncogenic signalling. *J. Biochem.* **157**, 431–438.

Padua, D. and Massagué, J. (2009). Roles of TGFβ in metastasis. *Cell Res.* **19**, 89–102.

Park, M. S., Kim, Y. H. and Lee, J. W. (2010). FAK mediates signal crosstalk between type II collagen and TGF-beta 1 cascades in chondrocytic cells. *Matrix Biol.* **29**, 135–142.

RB, I. and TJ, Y. (2000). Role of Src expression and activation in human cancer. *Oncogene* **19**, 5636–5642.

Ritchie, S., Boyd, F. M., Wong, J. and Bonham, K. (2000). Transcription of the human c-Src promoter is dependent on Sp1, a novel pyrimidine binding factor SPy, and can be inhibited by triplex-forming oligonucleotides. *J. Biol. Chem.* **275**, 847–854.

Shi, Y. and Massagué, J. (2003). Mechanisms of TGF-β signaling from cell membrane to the nucleus. *Cell* **113**, 685–700.

Sundqvist, A., Morikawa, M., Ren, J., Vasilaki, E., Kawasaki, N., Kobayashi, M., Koinuma, D., Aburatani, H., Miyazono, K., Heldin, C. H., et al. (2018). JUNB governs a feed-forward network of TGFβ signaling that aggravates breast cancer invasion. *Nucleic Acids Res.* **46**, 1180–1195.

Sundqvist, A., Vasilaki, E., Voytyuk, O., Bai, Y., Morikawa, M., Moustakas, A., Miyazono, K., Heldin, C. H., ten Dijke, P. and van Dam, H. (2020). TGFβ and EGF signaling orchestrates the AP-1- and p63 transcriptional regulation of breast cancer invasiveness. *Oncogene* **39**, 4436–4449.

Tanaka, K., Ito, Y., Kajiwara, K., Nada, S. and Okada, M. (2020). Ubiquitination of Src promotes its secretion via small extracellular vesicles. *Biochem. Biophys. Res. Commun.* **525**, 184–191.

Tsai, C. C., Kuo, F. T., Lee, S. B., Chang, Y. T. and Fu, H. W. (2019). Endocytosis-dependent lysosomal degradation of Src induced by protease-activated receptor 1. *FEBS Lett.* **593**, 504–517.

Tsukamoto, T., Kajiwara, K., Nada, S. and Okada, M. (2019). Src mediates TGF-β-induced intraocular pressure elevation in glaucoma. *J. Cell. Physiol.* **234**, 1730–1744.

Verbeek, B. S., Vroom, T. M., Adriaansen-Slot, S. S., Ottenhoff-Kalff, A. E., Geertzema, J. G. N., Hennipman, A. and Rijksen, G. (1996). c-Src protein expression is increased in human breast cancer. An immunohistochemical and biochemical analysis. *J. Pathol.* **180**, 383–388.

Vincent, T., Neve, E. P. A., Johnson, J. R., Kukalev, A., Rojo, F., Albanell, J., Pietras, K., Virtanen, I., Philipson, L., Leopold, P. L., et al. (2009). A SNAIL1-SMAD3/4 transcriptional repressor complex promotes TGF-β mediated epithelial-mesenchymal transition. *Nat. Cell Biol.* **11**, 943–950.

Wang, N., Liang, H., Zhou, Y., Wang, C., Zhang, S., Pan, Y., Wang, Y., Yan, X., Zhang, J., Zhang, C. Y., et al. (2014). miR-203 suppresses the proliferation and migration and promotes the apoptosis of lung cancer cells by targeting SRC. *PLoS One* **9**,.

Webb, D. J., Donais, K., Whitmore, L. A., Thomas, S. M., Turner, C. E., Parsons, J. T. and Horwitz, A. F. (2004). FAK-Src signalling through paxillin, ERK and MLCK regulates adhesion disassembly. *Nat. Cell Biol.* **6**, 154–161.

Westhoff, M. A., Serrels, B., Fincham, V. J., Frame, M. C. and Carragher, N. O. (2004). Src-Mediated Phosphorylation of Focal Adhesion Kinase Couples Actin and Adhesion Dynamics to

Survival Signaling. *Mol. Cell. Biol.* **24**, 8113–8133.

Wiener, J. R., Windham, C., Estrella, V. C., Parikh, N. U., Thall, P. F., Deavers, M. T., Bast, R. C., Mills, G. B. and Gallick, G. E. (2003). Activated Src protein tyrosine kinase is overexpressed in late-stage human ovarian cancers. *Gynecol. Oncol.* **88**, 73–79.

Yakymovych, I., Yakymovych, M., Hamidi, A., Landström, M. and Heldin, C. H. (2022). The type II TGF-β receptor phosphorylates Tyr182 in the type I receptor to activate downstream Src signaling. *Sci. Signal.* **15**, 1–15.

Yeatman, T. J. (2004). A renaissance for SRC. *Nat. Rev. Cancer* **4**, 470–480.

Figures

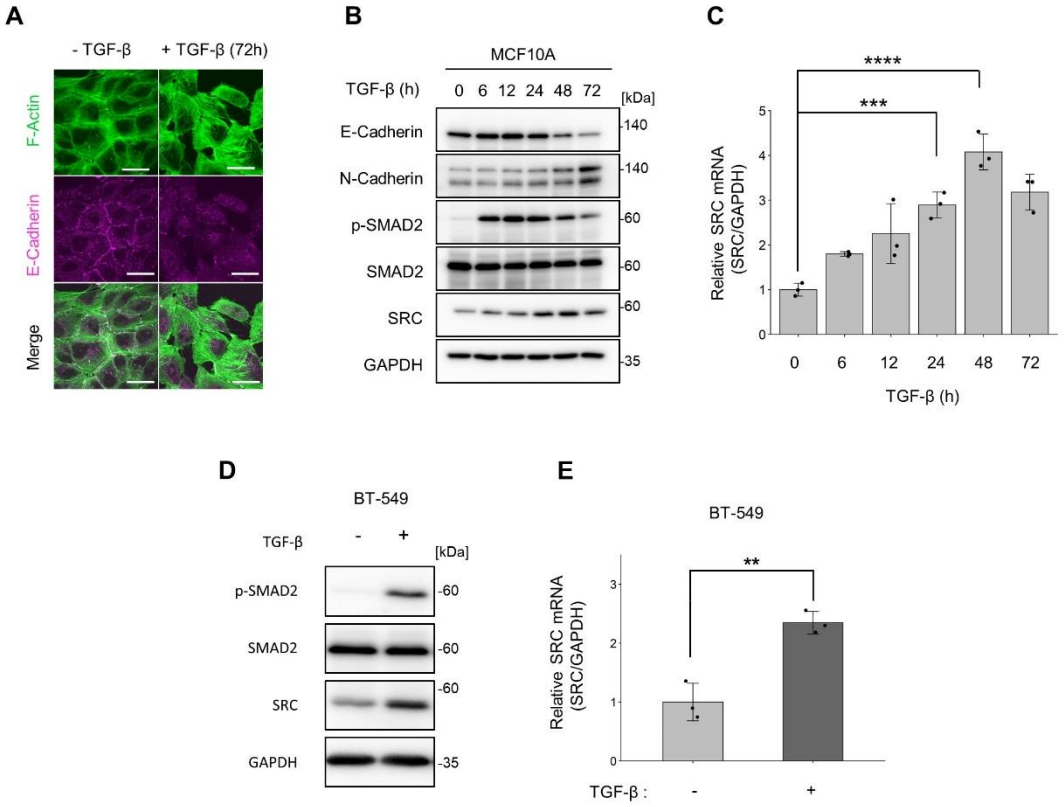

Figure 1. TGF-β stimulation upregulates *SRC* transcription in MCF10A and BT-549.
(A) MCF10A cells were treated with TGF-β1 (10 ng/ml) for 72h. The cells were subjected to immunofluorescence staining for F-actin and E-cadherin. The scale bar represents 10 μm. (B, C) MCF10A cells were treated with TGF-β1(10 ng/ml) for the indicated times. (B) Cell lysates were subjected to immunoblotting using the indicated antibodies. (C) Total RNA was isolated and subjected to qPCR. Relative expression levels were calculated using the mean value at 0h. (D, E) triple-negative breast cancer cell line BT-549 was treated with TGF-β1 (10 ng/ml) for 24h. (D) Cell lysates were subjected to immunoblotting using the indicated antibodies. (E) Total RNA was isolated and subjected to qPCR. (C and E) The mean ratios ± SDs were obtained from three independent experiments. ** $p < 0.01$; ***, $p < 0.001$; ****, $p < 0.0001$; N.S., not significantly different; One-way ANOVA with Tukey's post hoc test in (C); Unpaired two-tailed *t*-test. in (E).

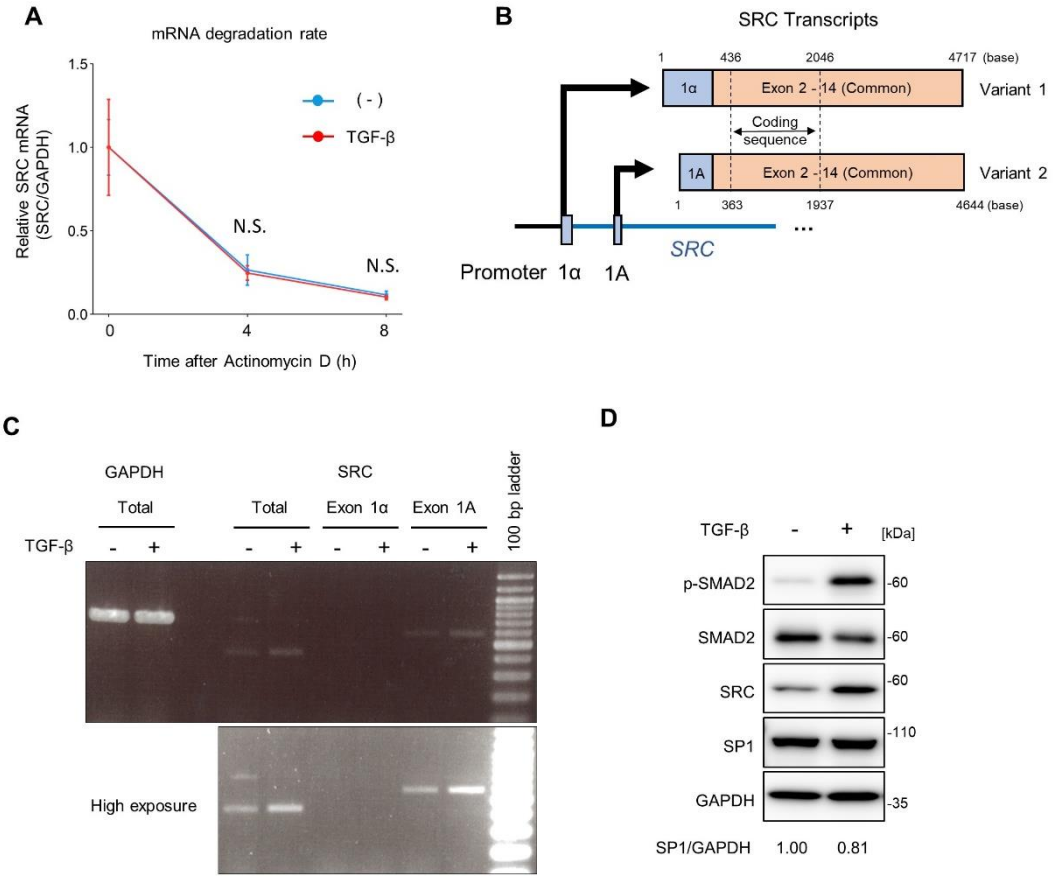

Figure 2. Characterization of TGF-β-induced SRC expression.

(A) MCF10A cells were treated with actinomycin D (10 μg/ml) for 4 or 8 h in the presence or absence of TGF-β1(10 ng/ml). TGF-β stimulation was conducted for 24 h, and then subjected to quantitative real-time PCR. Relative expression levels were calculated using the mean value at 0 h. (B) Schematic diagram of the transcriptional variants of SRC mRNA. Each variant is regulated by two different promoters and contains different exon1. (C) Transcriptional variants of SRC mRNA were analyzed by real-time PCR. (D) Immunoblotting analysis for the expression of SP1 in MCF10A cells. (C and D) MCF10A cells were treated with TGF-β1 (10 ng/ml) for 24 h. (A) The mean ratios ± SDs were obtained from three independent experiments. N.S., not significantly different; One-way ANOVA with Tukey's post hoc test.

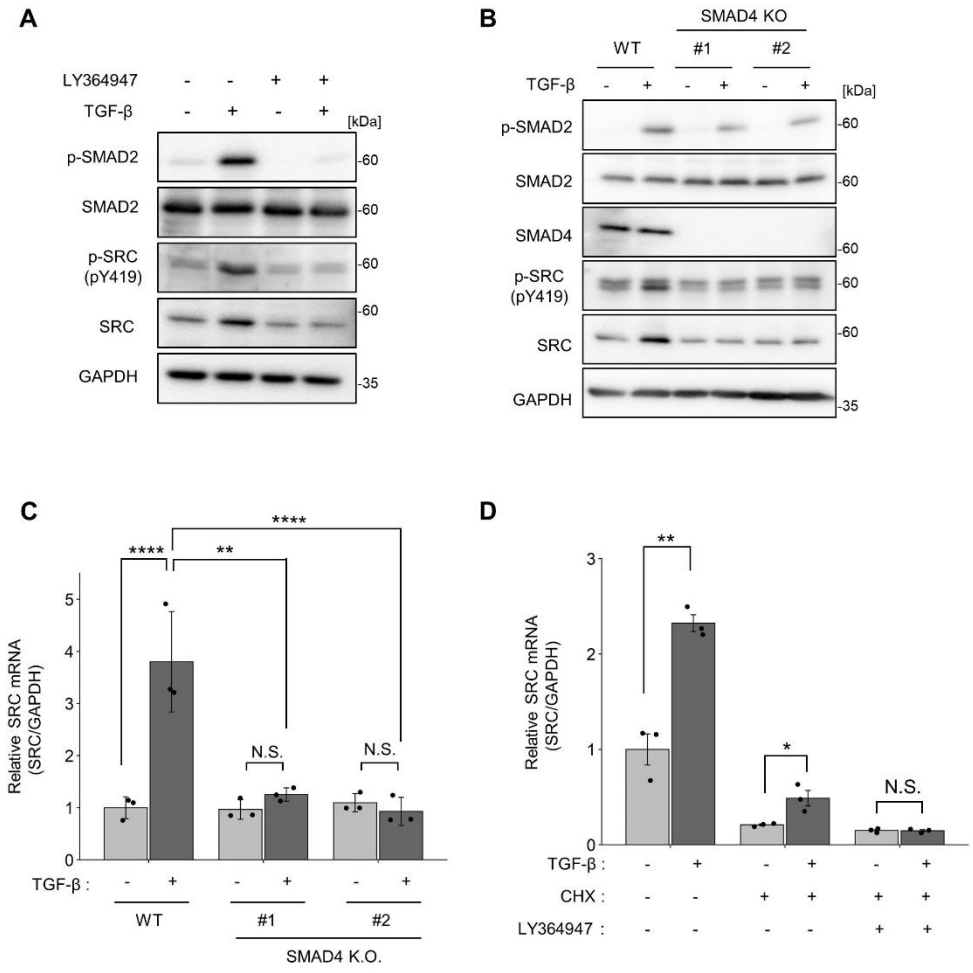

Figure 3. SRC expression is directly regulated by the TGF-β/SMAD pathway.

(A) MCF10A cells were treated with or without TGF-β1 (10 ng/ml) and the TGFβRI inhibitor LY364947 (2 μM) for 24 h. Cell lysates were subjected to immunoblotting using the indicated antibodies. (B, C) Wild-type and SMAD4-knockout clones were treated with TGF-β1 (10 ng/ml) for 24 h. (B) Cell lysates were subjected to immunoblotting using the indicated antibodies. (C) Total RNA was isolated and subjected to qPCR. (D) MCF10A cells were pretreated with cycloheximide (10 μg/ml) for 2 h, and then treated with or without TGF-β1 (10 ng/ml) and TGFβRI inhibitor LY364947 (2 μM) for 8 h. Total RNA was isolated and subjected to quantitative real-time polymerase chain reaction PCR. (C and D) The mean ratios ± SDs were obtained from three independent experiments. *, $p < 0.05$; **, $p < 0.01$; N.S., not significantly different; One-way ANOVA with Tukey's post hoc test in (C); Unpaired two-tailed *t*-test in (D).

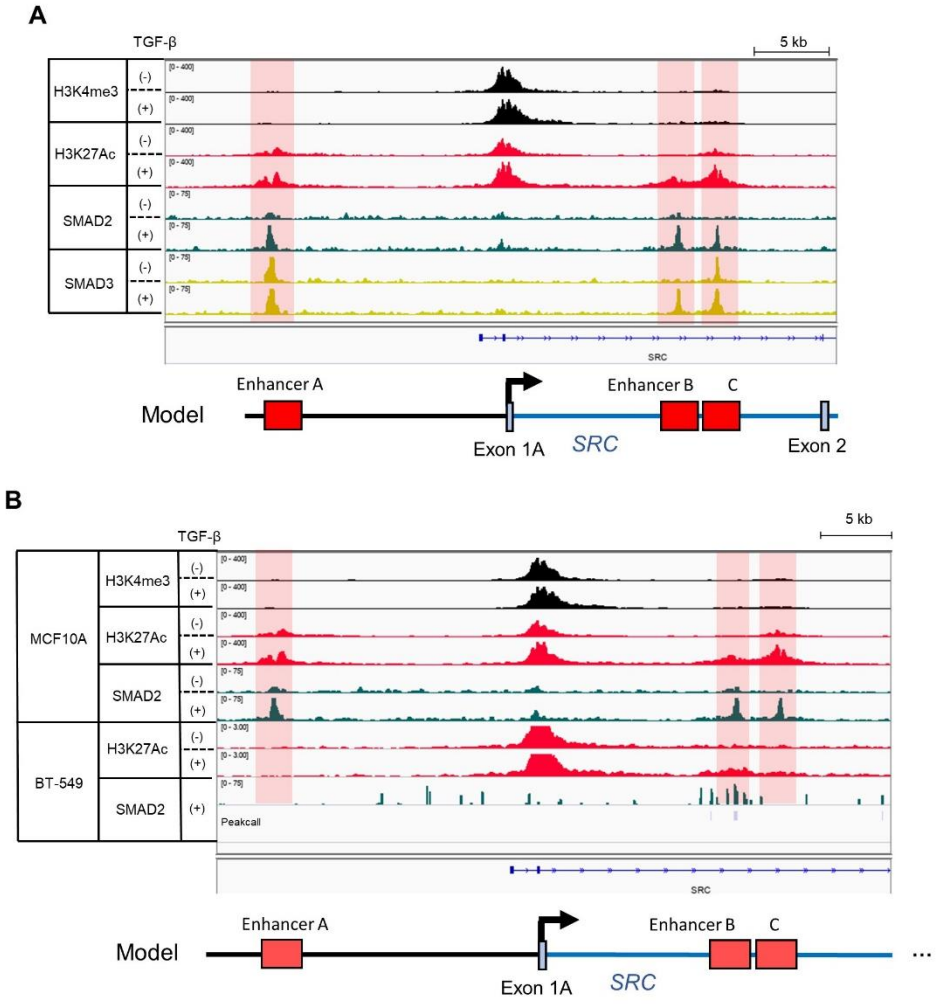

Figure 4. Histone modifications and SMAD2/3 localization at the *SRC* promoter.

(A) Genomic loci of *the SRC* promoter region in MCF10A. The IP targets are H3K4me3 (black), H3K27Ac (red), SMAD2 (green), and SMAD3(yellow). The ChIP-Seq results were visualized using IGV. (B) Genomic loci of the *SRC* promoter region in BT-549. The IP targets are H3K4me3 (black), H3K27Ac (red), and SMAD2 (green). The ChIP-Seq results in MCF10A and BT-549 cells were visualized using IGV. Peak call analysis was conducted using the findPeaks program in HOMER.

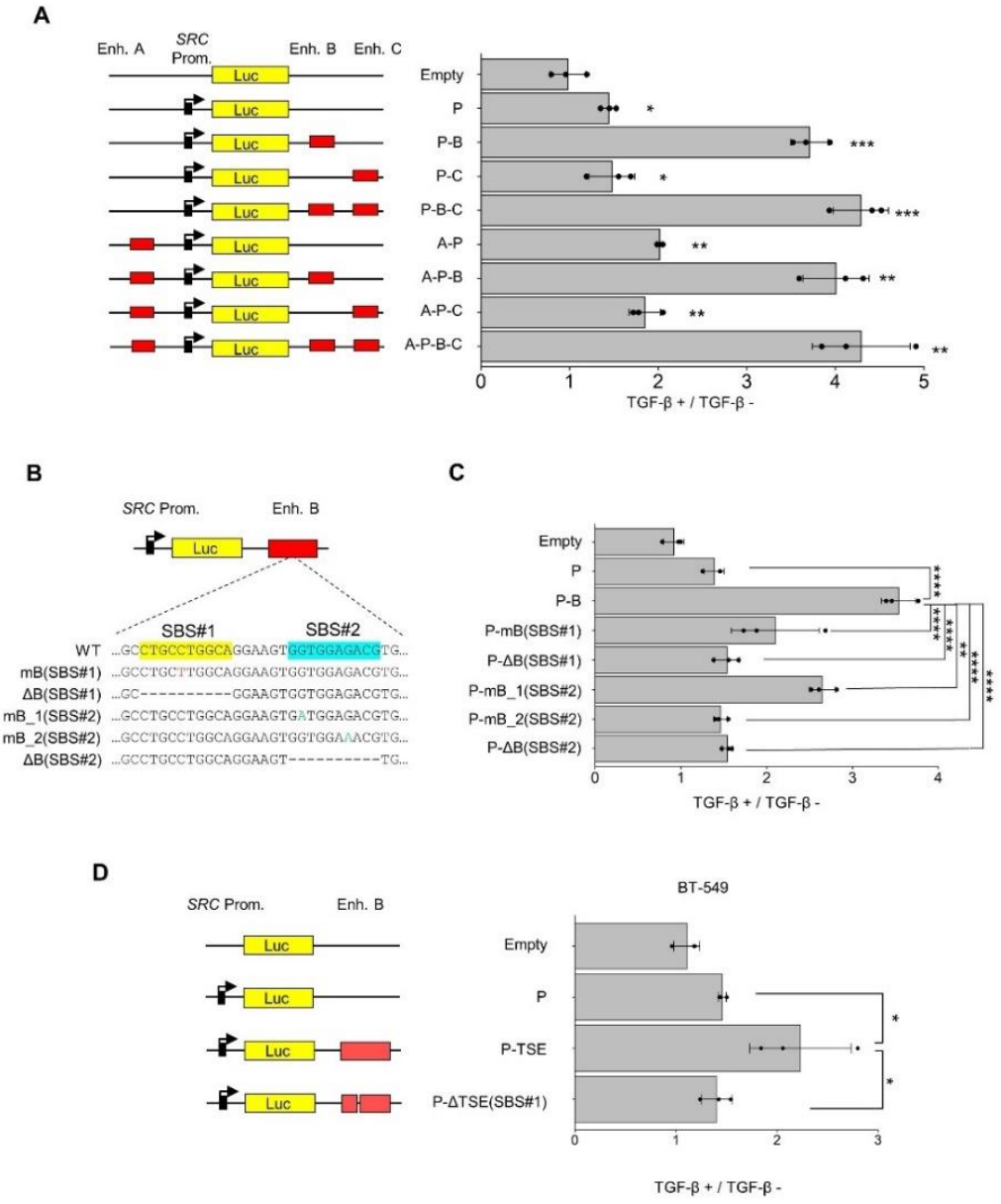

Figure 5. A TGF-β-responsive SRC intragenic enhancer increases *SRC* promoter activity.

(A) Schematic diagram of the F-luciferase reporter vectors is shown on the left, and the result of the luciferase reporter assay is shown on the right. The reporter and internal control vectors were co-transfected in MCF10A cells overnight, and then transfected cells were treated with TGF-β1 (10 ng/ml) for 24 h. Cell lysates were subjected to a luciferase reporter assay. Each data point was normalized to the luminescence of the untreated samples. (B) Schematic diagram of SBS-mutant vector constructs. (C) Luciferase reporter assay was conducted using mutant vectors in MCF10A cells.

Each data point was normalized to the luminescence of the untreated samples. (D) Luciferase reporter assay was conducted using the SBS mutant vector in BT-549 cells. Each data point was normalized to the luminescence of the untreated samples. (A, C, and D) The mean ratios ± SDs were obtained from three independent experiments. *, $p < 0.05$; **, $p < 0.01$; ***, $p < 0.001$; ****, $p < 0.0001$; Unpaired two-tailed *t*-test in (A); One-way ANOVA with Tukey's post hoc test in (C and D).

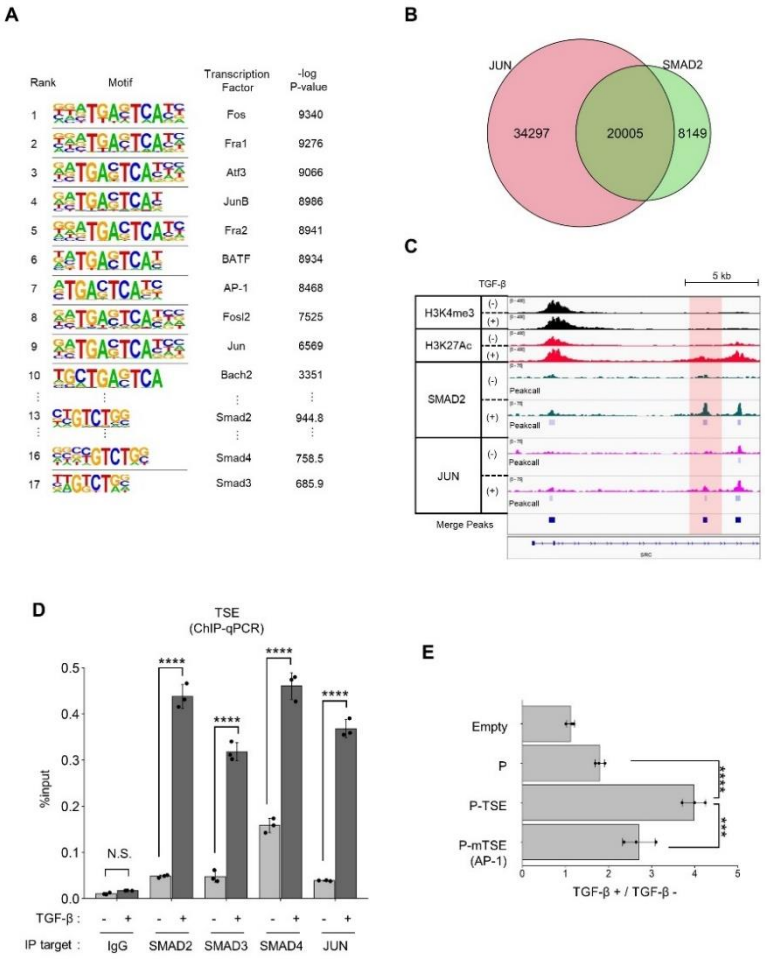

Figure 6. JUN is required for TSE-mediated SRC promoter activation.

(A) Motifs enriched in the SMAD complex binding site in TGF-β-stimulated MCF10A cells. (B) Comparison of the locus of JUN binding sites and SMAD complex binding sites. (C) Genomic loci of *the SRC* promoter region. The IP targets are H3K4me3 (black), H3K27Ac (red), SMAD2 (green), and JUN (magenta). The ChIP-Seq results were visualized using IGV. Peak call analysis was conducted using the findPeaks program in HOMER. (D) ChIP assay was conducted using IgG control or antibodies targeting SMAD2, SMAD3, SMAD4, and JUN. The TSE region was quantified using qPCR. (E) Result of the luciferase reporter assay. Reporter and internal control vectors co-transfected in MCF10A overnight, and transfected cells were treated with TGF-β1 (10 ng/ml) for 24 h. Cell lysates were subjected to a luciferase reporter assay. Each data point was normalized to the luminescence of the untreated samples. (D and E) The mean ratios ± SDs were obtained from three independent experiments. **, $p < 0.01$; ***, $p < 0.001$; ****, $p < 0.0001$; Unpaired two-tailed *t*-test in (D); One-way ANOVA with Tukey's post hoc test in (E).

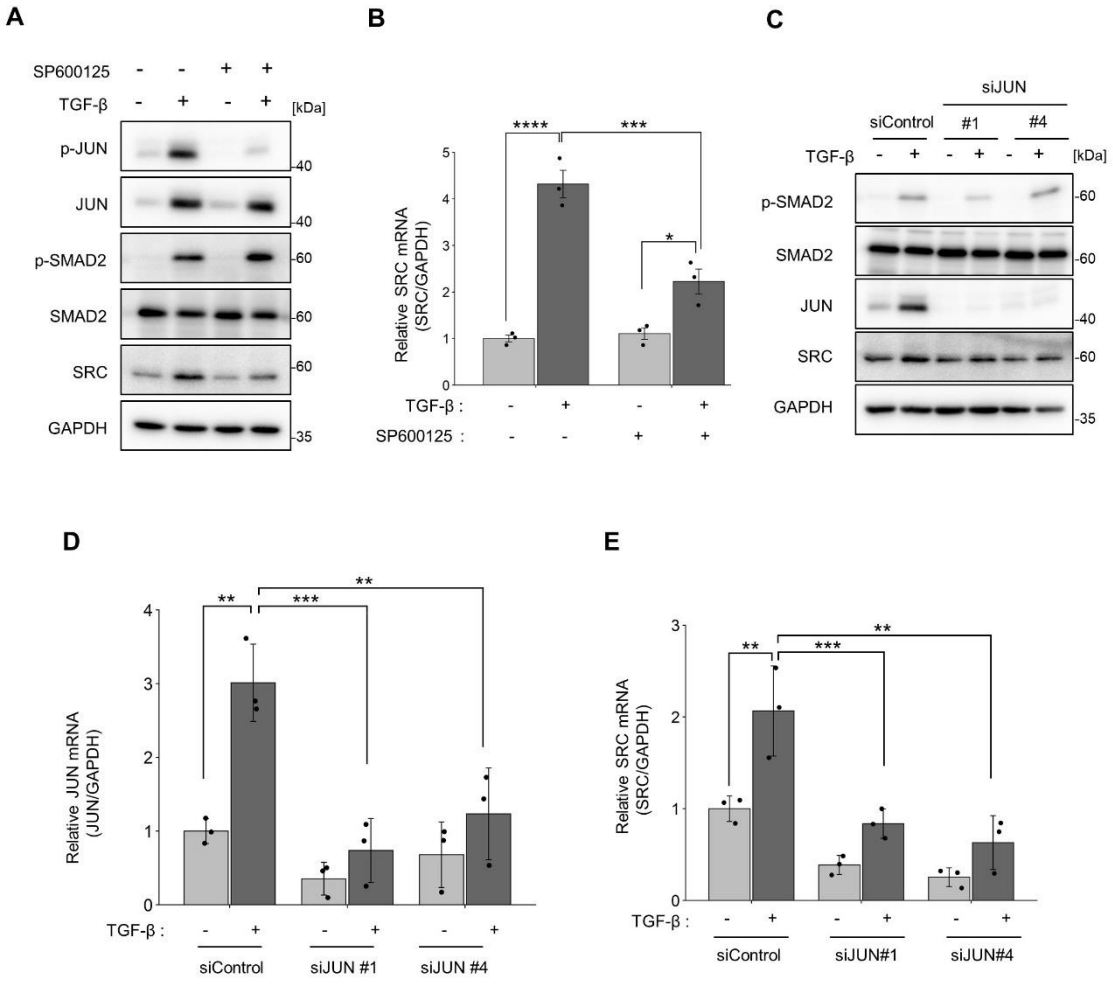

Figure 7. SRC expression is regulated by the TGF-β/JNK/JUN pathway.

(A, B) MCF10A cells were treated with or without TGF-β1 (10 ng/ml) and SP600125 (20 μM) for 24h. (A) Cell lysates were subjected to immunoblotting using the indicated antibodies. (B) Total RNA was isolated and subjected to qPCR analysis. (C, D, and E) MCF10A cells were treated with the indicated siRNAs overnight and then with or without TGF-β1(10 ng/ml) for 24h. (C) Cell lysates were subjected to immunoblotting using the indicated antibodies. (D, E) Total RNA was isolated and subjected to quantitative real-time polymerase chain reaction PCR. (B, D, and E) The mean ratios ± SDs were obtained from three independent experiments. **, $p < 0.01$; ***, $p < 0.001$; ****, $p < 0.0001$; One-way ANOVA with Tukey's post hoc test in (B, D and E).

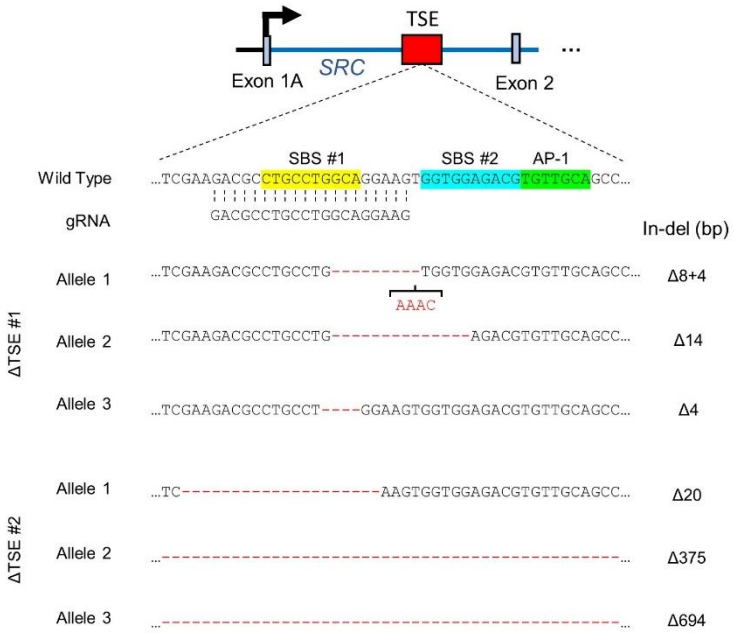

Figure 8. DNA sequences in ΔTSE MCF10A cell lines.

Schematic diagram of CRISPR/Cas9-based mutagenesis of TSE. The DNA sequences in TSE mutant clones are shown in the middle and bottom.

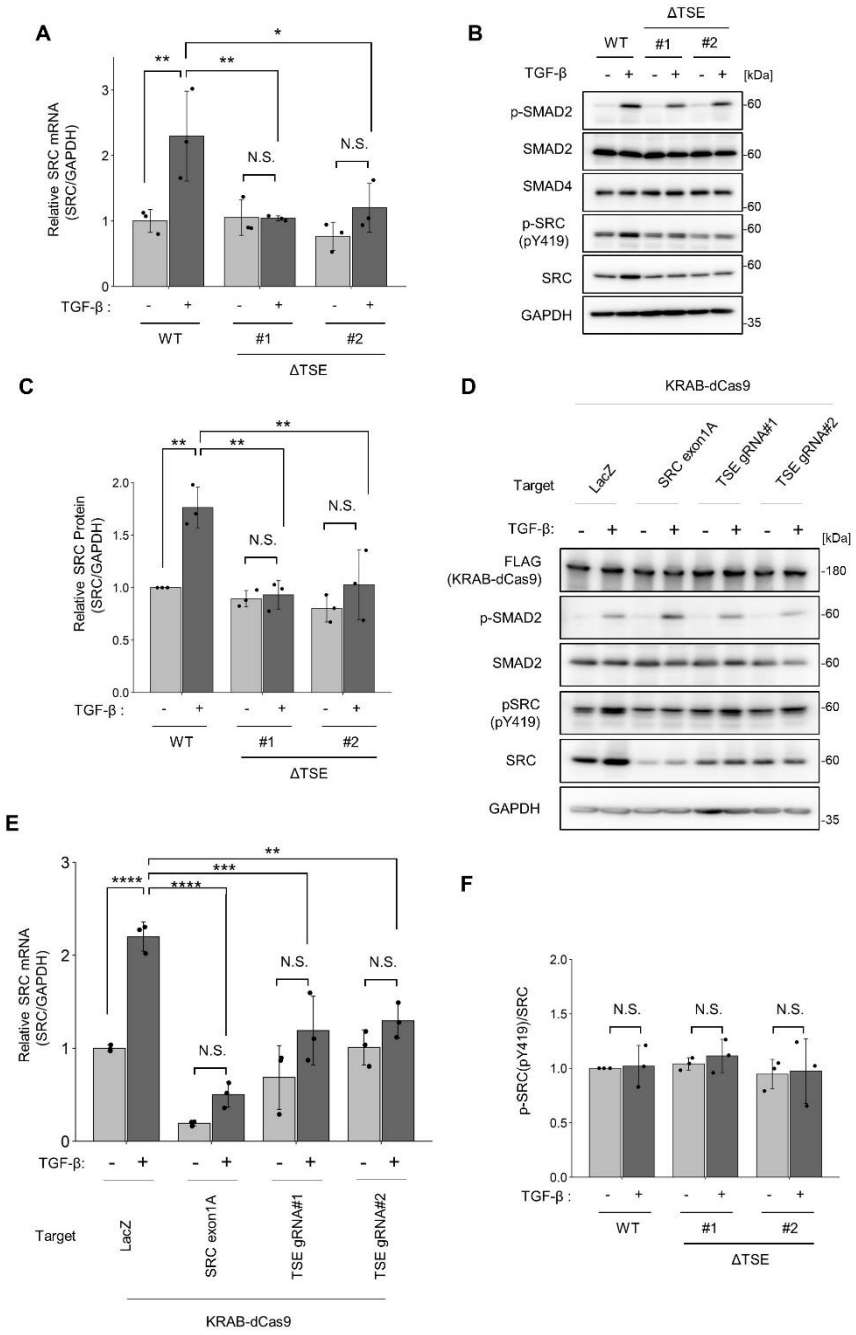

Figure 9. TGF-β-induced SRC expression and activation are suppressed by the TSE mutation and CRISPRi-based enhancer inhibition.

(A, B) Wild-type MCF10A cells and ΔTSE clones were treated with TGF-β1(10 ng/ml) for 24h. (A) Total RNA was isolated and subjected to qPCR. (B) Cell lysates were subjected to immunoblotting using the indicated antibodies. (C) Quantification of SRC protein levels in the immunoblot analysis shown in (B). (D, E) Indicated gRNAs are expressed in KRAB-dCas9 expressing MCF10A. Cells

were treated with TGF-β1 (10 ng/ml) for 24 h. (D) Cell lysates were subjected to immunoblotting using the indicated antibodies. (E) Total RNA was isolated and subjected to qPCR. (F) Quantification of SRC-pY419 in the immunoblot analysis shown in (B). (A, C, E, and F) The mean ratios ± SDs were obtained from three independent experiments. *, $p < 0.05$; **, $p < 0.01$; ***, $p < 0.001$; ****, $p < 0.0001$; N.S., not significantly different; One-way ANOVA with Tukey's post hoc test.

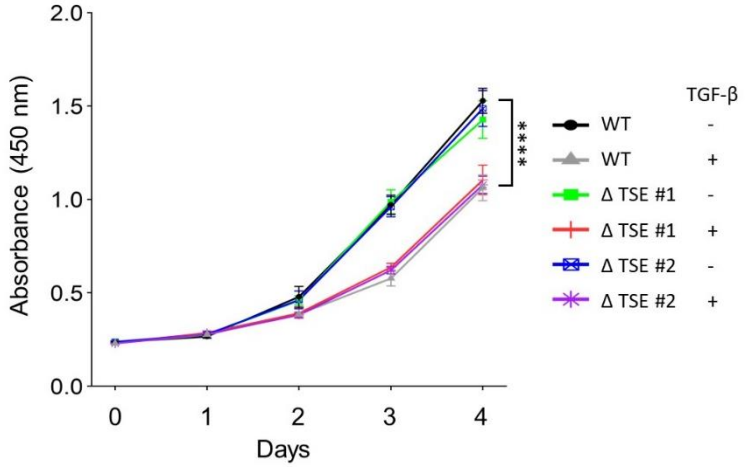

Figure 10. TGF-β reduced cell proliferation rate in WT and ΔTSE cell lines.

Wild-type MCF10A cells and ΔTSE clones were treated with TGF-β1 (10 ng/ml). WST-8 was added at the indicated time points and the cells were incubated for 1h. Mean ratios ± SDs were obtained from five biologically independent samples. Representative results from three independent experiments are shown. ****, $p < 0.0001$; Unpaired two-tailed *t*-test.

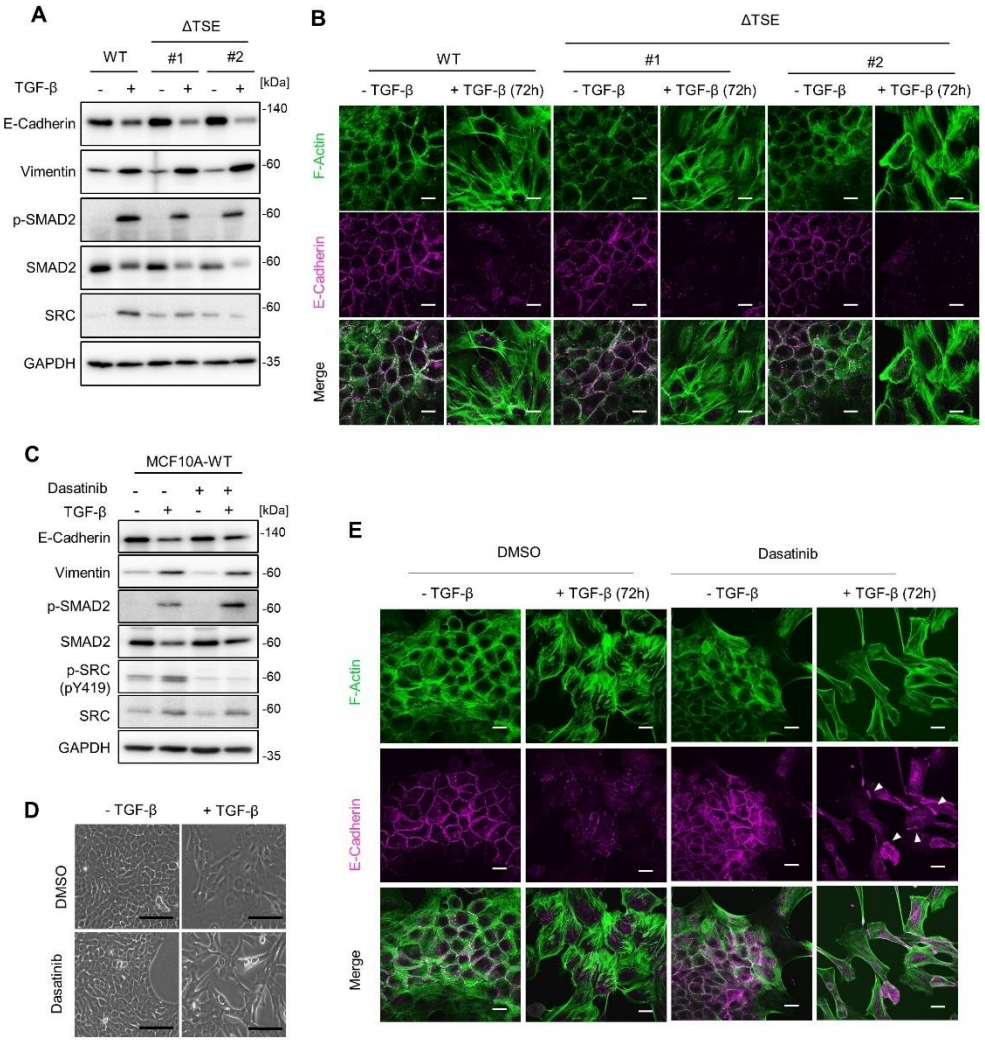

Figure 11. The effect of the TSE mutation or SRC inhibition on TGF-β-induced gene expression and EMT-associated morphological change

(A, B) Wild-type MCF10A cells and ΔTSE clones were treated with TGF-β1 (10 ng/ml) for 72 h. (A) Cell lysates were subjected to immunoblotting using the indicated antibodies. (B) Cells were subjected to immunofluorescence staining for F-actin and E-cadherin expression. The scale bar represents 10 μm. (C-E) wild-type MCF10A cells were treated with TGF-β1 (10 ng/ml) in the presence or absence of dasatinib (0.1 μM) for 72 h. (C) Cell lysates were subjected to immunoblotting using the indicated antibodies. (D) Cell morphology observed by phase contrast microscopy. The scale bar represents 20 μm. (E) Cells were subjected to immunofluorescence staining for F-actin and E-cadherin expression. White arrowheads indicate the accumulation of E-cadherin. The scale bar represents 10 μm.

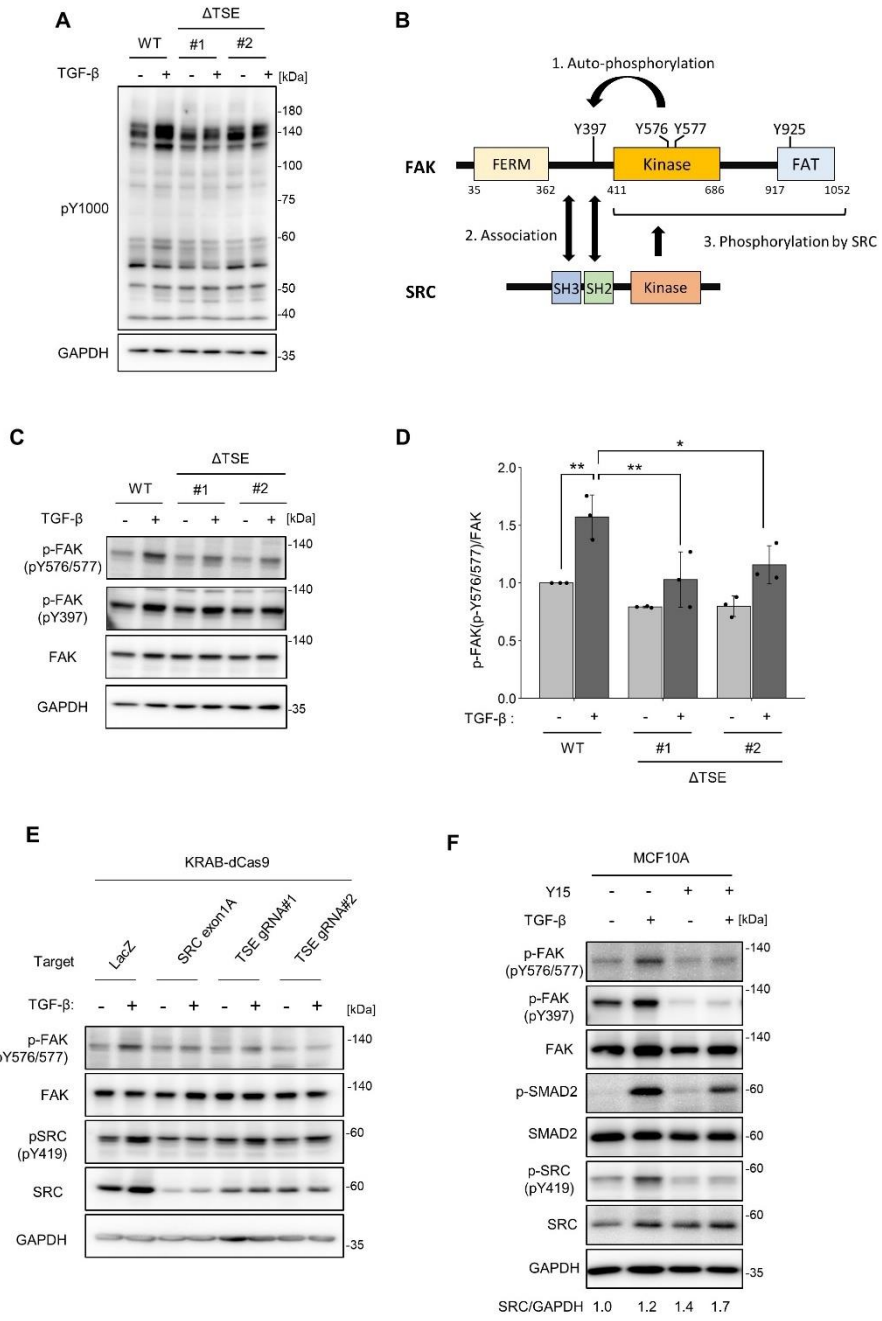

Figure 12. Inhibition of the TSE activity attenuates the SRC-mediated FAK phosphorylation.

(A) Wild-type MCF10A cells and ΔTSE clones were treated with TGF-β1(10 ng/ml) for 24h. Cell lysates were subjected to immunoblotting using the indicated antibodies. (B) Schematic diagram of the interactions between FAK and SRC. (C) Wild-type MCF10A cells and ΔTSE clones were treated with TGF-β1 (10 ng/ml) for 24 h. Cell lysates were subjected to immunoblotting using the indicated

antibodies. (D) Quantification of FAK-pY576/577 level in immunoblot analysis shown in (C). (E) Indicated gRNAs are expressed in KRAB-dCas9 expressing MCF10A. Cells were treated with TGF-β1(10 ng/ml) for 24 h. Cell lysates were subjected to immunoblotting using the indicated antibodies. (F) MCF10A cells were treated with or without TGF-β1(10 ng/ml) and the FAK inhibitor Y15 (10 μM) for 24 h. Cell lysates were subjected to immunoblotting using the indicated antibodies. (D) The mean ratios ± SDs were obtained from three independent experiments. *, $p < 0.05$; **, $p < 0.01$; One-way ANOVA with Tukey's post hoc test.

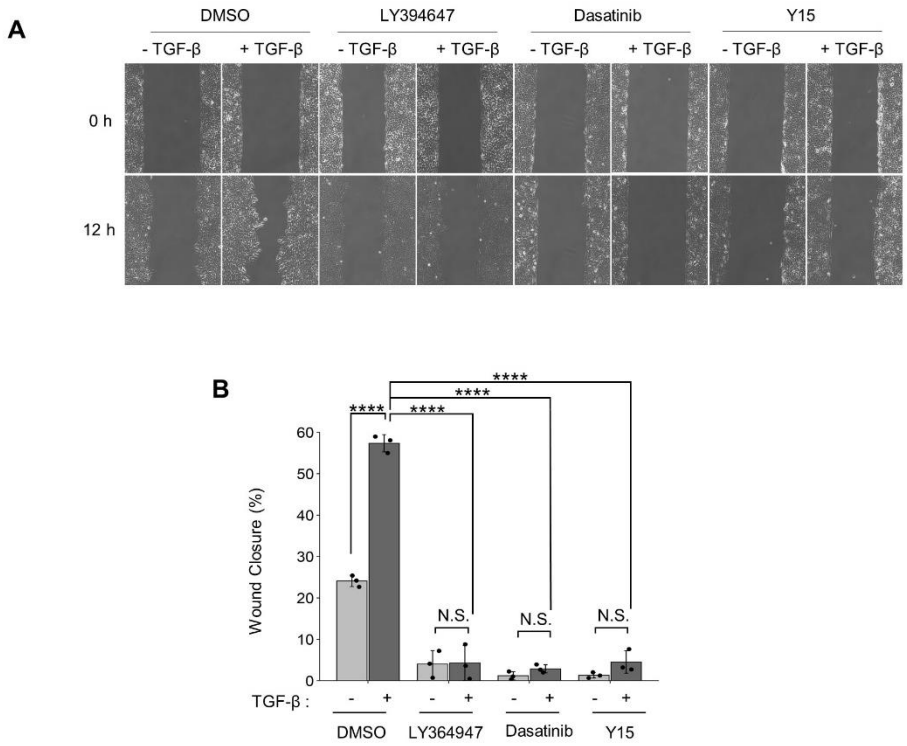

Figure 13. The effect of the TβRI, SRC, and FAK inhibitors on the EMT-associated cell motility in MCF10A.

(A) Wound healing assay of wild-type MCF10A cells treated with or without TGF-β1 (10 ng/ml) in the presence or absence of DMSO, LY394647, dasatinib, or Y15 for 12 h. (B) Quantification of the wound closure rate using the images shown in (A). (B) The mean ratios ± SDs were obtained from three independent experiments. ****, $p < 0.0001$; N.S., not significantly different; One-way ANOVA with Tukey's post hoc test.

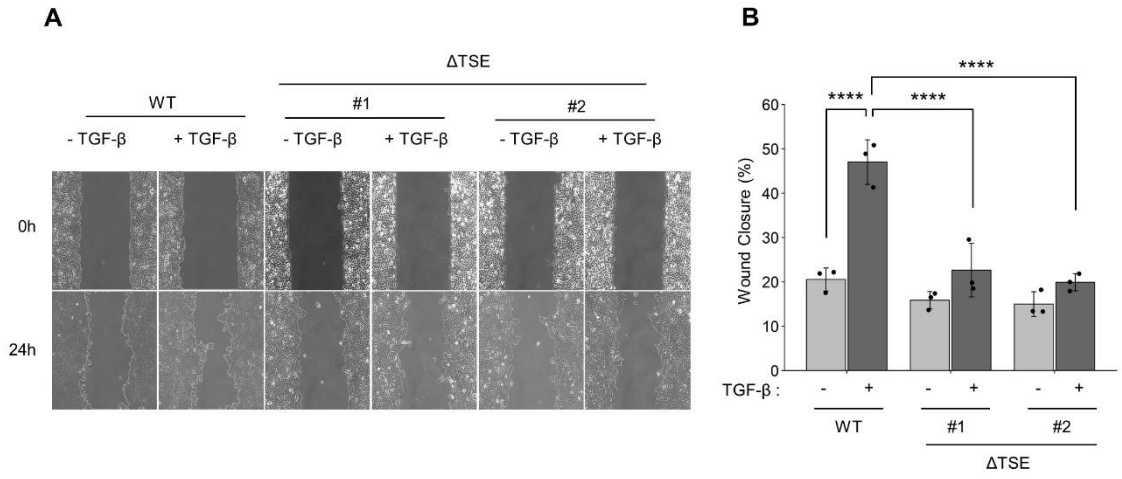

Figure 14. Deletion of the TSE attenuates EMT-associated cell motility.

(A) Wound healing assay of wild-type MCF10A cells and ΔTSE clones treated with or without TGF-β1 (10 ng/ml) for 24 h. (B) Quantification of the wound closure rate using the images shown in (A). (B) The mean ratios ± SDs were obtained from three independent experiments. ****, $p < 0.0001$; One-way ANOVA with Tukey's post hoc test.

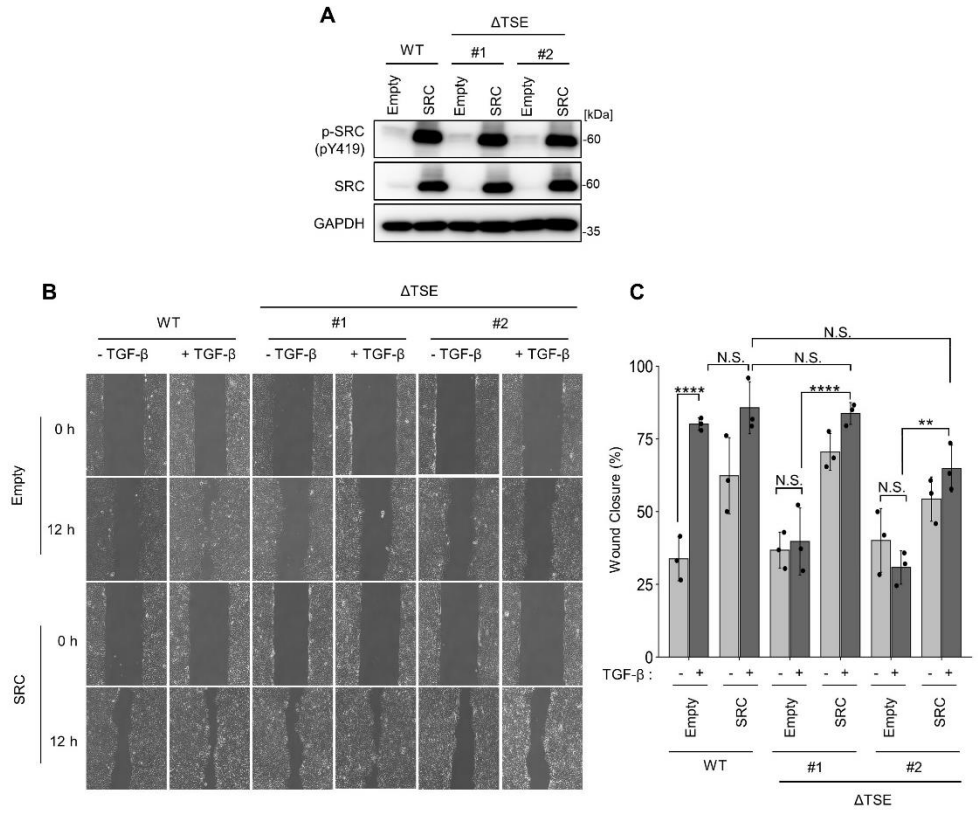

Figure 15. The effect of SRC overexpression on the EMT-associated cell motility in WT and ΔTSE cell lines.

(A) SRC is overexpressed in wild-type and ΔTSE MCF10A. Cell lysates were subjected to immunoblotting using the indicated antibodies. (B) Wound healing assay using SRC overexpressed MCF10A cells treated with or without TGF-β1 (10 ng/ml) for 12h. (C) Quantification of the wound closure rate using the images shown in (B). (C) The mean ratios ± SDs were obtained from three independent experiments. **, $p < 0.01$; ****, $p < 0.0001$; N.S., not significantly different; One-way ANOVA with Tukey's post hoc test.

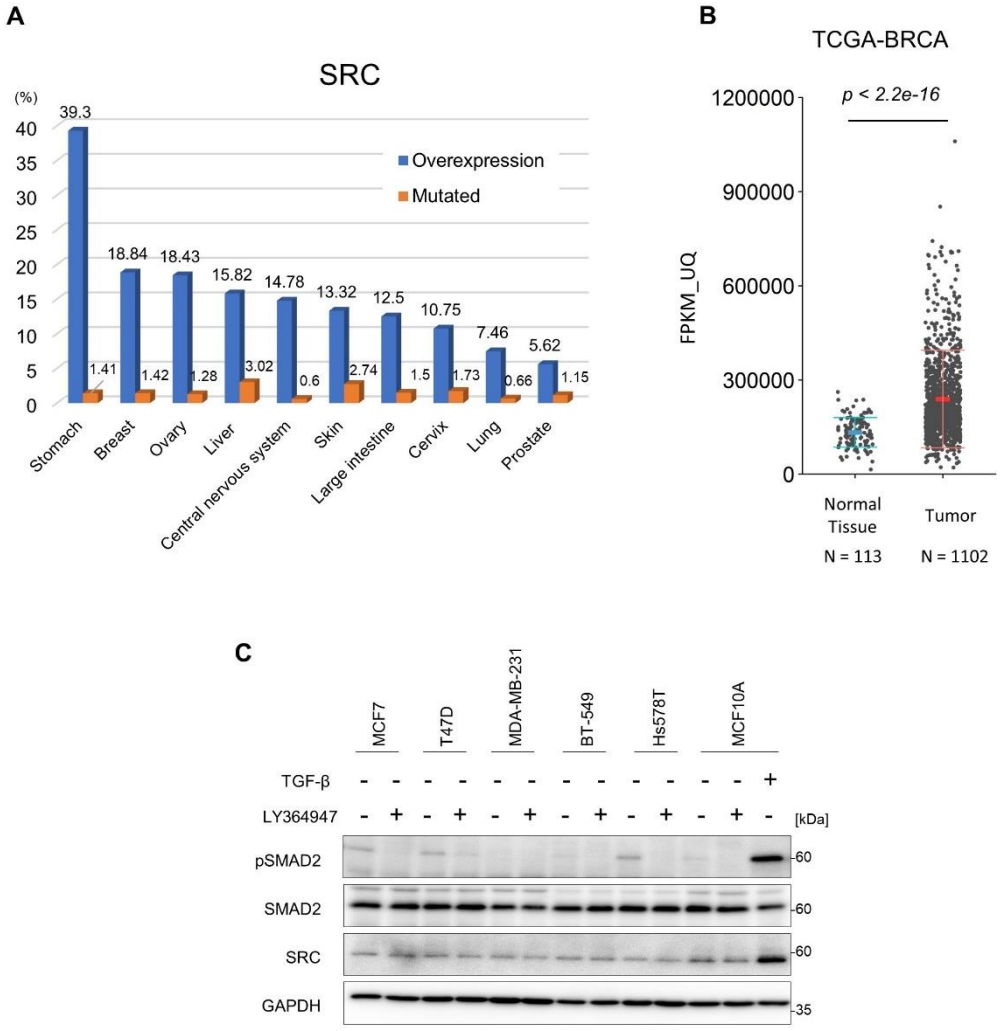

Figure 16. SRC is overexpressed in various human cancer types, but not in breast cancer cell lines.

(A) The frequencies of somatic mutations in *SRC* in various human cancers were obtained from the Catalogue of Somatic Mutations in Cancer (COSMIC; https://cancer.sanger.ac.uk/cosmic). Blue and orange bars indicate the ratios of overexpression and genetic mutations, respectively. (B) SRC mRNA expression was analyzed using a cohort of breast cancer patients from The Cancer Genome Atlas (TCGA-BRCA). The *p*-value was determined using the Wilcoxon rank-sum test. (C) Cells were treated with TGFβRI inhibitor LY364947 (2 μM) or TGF-β1(10 ng/ml) for 48h. Cell lysates were subjected to immunoblotting using the indicated antibodies.

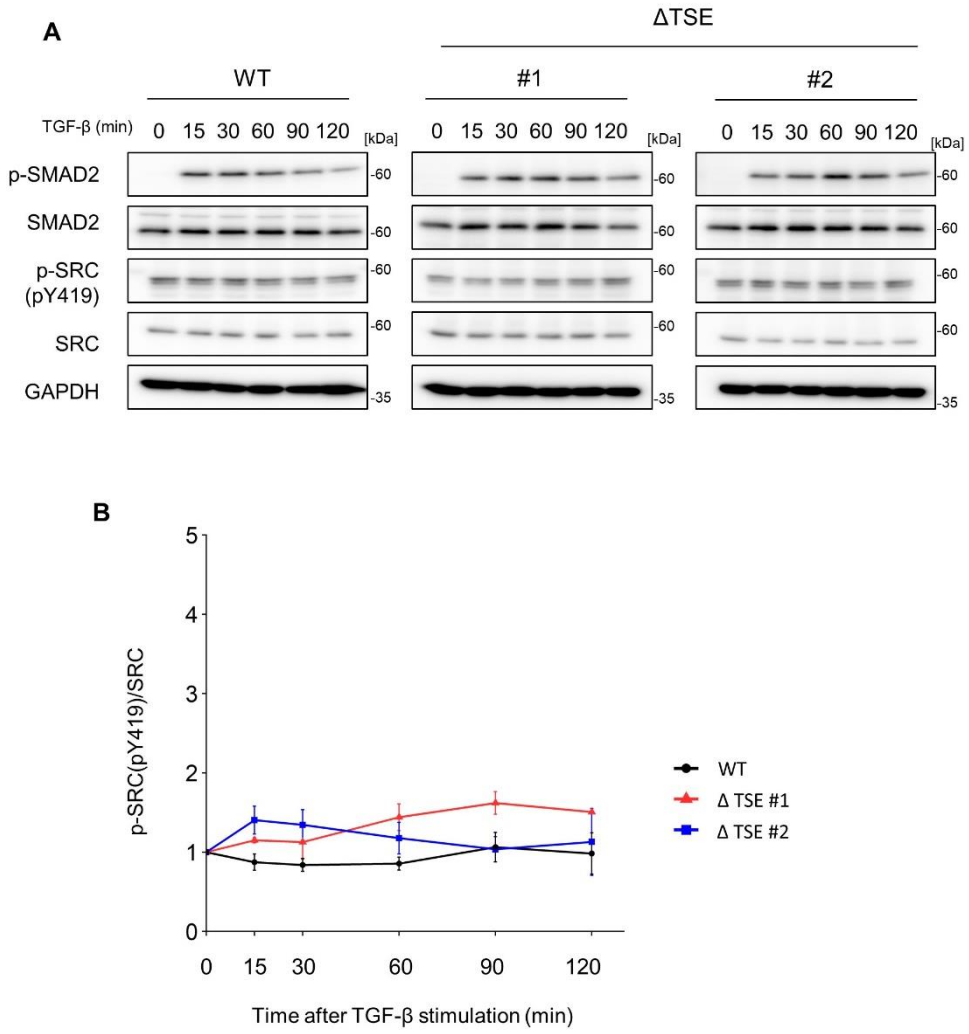

Figure 17. Short-time TGF-β stimulation in wild-type and ΔTSE cell lines.

(A, B) MCF10A cells were treated with TGF-β1 (5 ng/ml) for the indicated times. (A) Cell lysates were subjected to immunoblotting using the indicated antibodies. (B) Quantification of SRC-pY419 in the immunoblot analysis shown in (A). (B) The mean ratios ± SDs were obtained from three independent experiments.

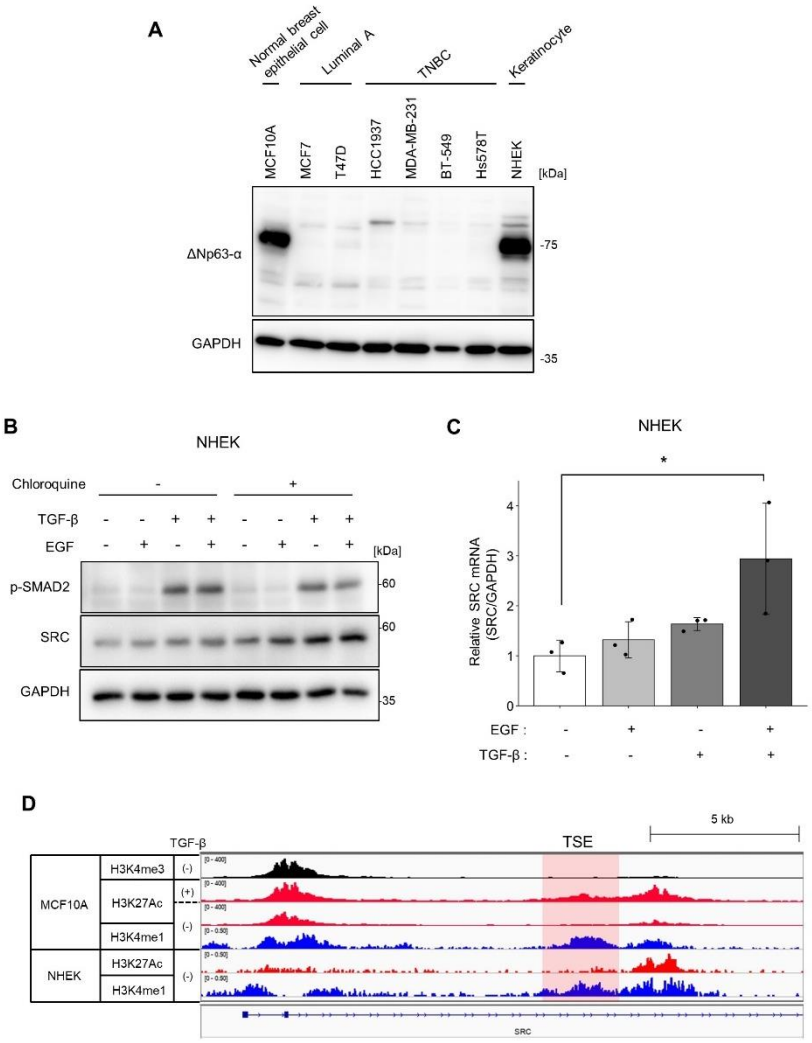

Figure 18. Co-stimulation of TGF-β and EGF regulates SRC expression in p63-expressing normal human epidermal keratinocytes (NHEK).

(A) Immunoblot analysis for the expression of p63 in the indicated cell lines. TNBC, triple-negative breast cancer. (B) NHEK cells were treated with TGF-β1 (10 ng/ml) and/or EGF (20 ng/ml) for 24h. Chloroquine (100 μM) was added to the medium, and the cells were incubated for 2 h before cell lysate collection. Cell lysates were subjected to immunoblotting using the indicated antibodies. (C) NHEK cells were treated with TGF-β1 (10 ng/ml) and/or EGF (20 ng/ml) for 24 h. Total RNA was isolated and subjected to quantitative real-time polymerase chain reaction PCR. (D) Genomic loci of *the SRC* promoter region in MCF10A and NHEK cells The IP targets are H3K4me3 (black), H3K27Ac (red), and H3K4me1 (blue). (C) Mean ratios ± SDs were obtained from three independent experiments. * $p < 0.05$; One-way ANOVA with Tukey's post hoc test.

Tables

Table 1. List of primers used for vector construction.

Cloning target		Sequence (5 ′→ 3 ′)
SRC 1A Promoter	Forward primer:	GTGAGGGGGCTGGGCTG
	Reverse primer:	CTGGGCCGGCGG
Enhancer. A	Forward primer:	GTTGTGGCAGGGAGGGGAG
	Reverse primer:	TACAAGAAAATGAGCCAGGCGTGG
Enhancer. B (TSE)	Forward primer:	AGTTGGCCATTTGCAGCGAG
	Reverse primer:	GCCACTTCCTCACAGAAAGCC
Enhancer. C	Forward primer:	GGCTTTCTGTGAGGAAGTGGC
	Reverse primer:	AGAACAGGTGTGGAGGAGGC
mTSE (SBS#1)	Forward primer:	ACGCCTGCTTGGCAGGAAGTGGTGGAGAC
	Reverse primer:	TCCTGCCAAGCAGGCGTCTTCGAGGAAAGG
ΔTSE (SBS#1)	Forward primer:	AAGACGCGGAAGTGGTGGAGACGTG
	Reverse primer:	CCACCACTTCCGCGTCTTCGAGGAAA
mTSE_1 (SBS#2)	Forward primer:	AGGAAGTGATGGAGACGTGTTGCAGCCC
	Reverse primer:	CGTCTCCATCACTTCCTGCCAGGCAGGCG
mTSE_2 (SBS#2)	Forward primer:	GGTGGAAACGTGTTGCAGCCCAAC
	Reverse primer:	CAACACGTTTCCACCACTTCCTGCC
ΔTSE (SBS#2)	Forward primer:	GGAAGTGGAGCCCAACTGGCAGATTC
	Reverse primer:	GTTGGGCTCCACTTCCTGCCAGGC
mTSE (AP-1)	Forward primer:	CGTGTTGCTGCCCAACTGGCAGATTCCC
	Reverse primer:	AGTTGGGCAGCAACACGTCTCCACCACTTC
Human SRC gene	Forward primer:	ATGGGTAGCAACAAGAGCAAGC
	Reverse primer:	CTAGAGGTTCTCCCCGGGCTGG

Table 2. List of siRNAs.

Target gene		Sequence (5 ′→ 3 ′)
si*JUN* #1	Sense	GAUGGAAACGACCUUCUAU[dT][dT]
	Antisense	AUAGAAGGUCGUUUCCAUC[dT][dT]
si*JUN* #4	Sense	GGCCCUGAAGGAGGAGCCU[dT][dT]
	Antisense	AGGCUCCUCCUUCAGGGCC[dT][dG]

Table 3. List of qPCR primers.

Target gene		Sequence (5 ′→ 3 ′)
SRC	Forward primer:	TCAACAACACAGAGGGAGAC
	Reverse primer:	CGTAGTTGCTGGGGATGTAG
GAPDH	Forward primer:	GCTCTCTGCTCCTCCTGTTC
	Reverse primer:	CGCCCAATACGACCAAATCC
JUN	Forward primer:	ACGACCTTCTATGACGATGCC
	Reverse primer:	CCAGGTTCAGGGTCATGCTC
(For Semi-qPCR in Fig. 1*E*)		
SRC Exon1A	Forward primer:	GTCTGCCCGTCCCGCTGGAC
SRC Exon1α	Forward primer:	AGCACAACCTGACCATCCTCACACTG
SRC Common	Forward primer:	GAAACCAGATGAGGACGCTGAGGCC
	Reverse primer:	AAAGGTGGTCACTCCACCGGCC
GAPDH	Forward primer:	CATCTTCCAGGAGCGAGATCCC
	Reverse primer:	TTCGTTGTCATACCAGGAAATGAGC
(For ChIP-qPCR in Fig. 4B)		
TSE	Forward primer:	CTGTCCATCCTTTCCTCGAA
	Reverse primer:	CTTGGGAATCTGCCAGTTG

Table 4. List of gRNA sequences and genotyping primers.

gRNA target		Sequence (5 ′→ 3 ′)
SMAD4		TCTGTCGATGCACGATTACT
Enhancer. B (TSE)		GACGCCTGCCTGGCAGGAAG
LacZ		CGAATACGCCCACGCGATGG
SRC exon1A		TCCCGGCCCGGAATCCATTC
TSE #1		GACGCCTGCCTGGCAGGAAG
TSE #2		GAGACGTGTTGCAGCCCAAC
PCR target		
SMAD4 for genotyping	Forward primer:	GTTGCTGGAGGCTGTTGAAAC
	Reverse primer:	CCCCTCTCCCTCCTATGACAT
Enhancer. B for genotyping	Forward primer:	CTTCCTGGGGGAGGAGGTAC
	Reverse primer:	GCCACTTCCTCACAGAAAGCC

Acknowledgements

This study was conducted at the Department of Oncogene Research, Research Institute for Microbial Diseases, Osaka University.

I would like to express my sincere gratitude to Professor Masato Okada for his instruction and thoughtful suggestions. Without his support, I could not have completed my research. I am also grateful to Dr. Shigeyuki Nada for his helpful suggestions and fruitful discussions. I sincerely thank Dr. Kentaro Kajiwara for his valuable advice, discussions, and continuous encouragement. Finally, I would like to thank my family and all lab members for their constant help and support.